Matrix Matters: Context-Driven Metabolic Shifts in *Bacillus cereus* and *Bacillus subtilis*

Emilie Viktoria Skriver[1,a], Tessa Suzanne Canoy[1,a], Yuandong Sha[1], Morten Arendt Rasmussen[1,2], Bekzod Khakimov[1], Susanne Knøchel[1], Henriette Lyng Røder*[1]

1: Department of Food Science, University of Copenhagen, Copenhagen, Denmark

2: Copenhagen Studies on Asthma in Childhood, Herlev-Gentofte Hospital, University of Copenhagen, Copenhagen, Denmark

[a] Emilie Viktoria Skriver and Tessa Suzanne Canoy contributed equally to this work and share first authorship.

***Corresponding author:** **h.lyng.roeder@food.ku.dk**
Section for Microbiology and Fermentation
Rolighedsvej 26
DK-1958 Frederiksberg

Abstract

Spore-forming *Bacillus* species, including pathogenic *Bacillus cereus* and spoilage-associated *Bacillus subtilis*, are major contributors to foodborne illness and product degradation. Understanding their metabolic behaviour in diverse food matrices is essential for improving risk assessment, spoilage prediction, and fermentation control. This study integrates isothermal microcalorimetry and targeted metabolomics to characterize the metabolic activity of *B. cereus* and *B. subtilis* in five nutrient sources: Brain Heart Infusion (BHI) medium, oat drink, milk, pea hydrolysate, and a combined oat-pea matrix. Metabolic heat production was monitored for 24 hours at 30°C. In BHI, *B. cereus* exhibited a shorter lag phase (mean ± sd: 4.3 hours ± 0.8) than *B. subtilis* (7.9 hours ± 1.0) but produced less total heat. Across all food matrices, *B. subtilis* consistently generated more heat. The oat-pea matrix supported the highest growth rates, surpassing oat or pea alone, and showed sugar depletion and accumulation of organic acids, indicating enhanced carbohydrate metabolism. Free amino acid release was matrix- and species-specific: *B. subtilis* had increased levels in oat, while *B. cereus* did so in pea. While *B. cereus* was metabolically active in all matrices, cereulide levels were matrix-dependent: 47.3 ± 1.7 ng/mL in oat, 3.0 ± 0.1 ng/mL in oat–pea, and undetectable in pea. These findings reveal clade-specific and matrix-driven metabolic strategies. This is the first study to combine calorimetry and metabolomics to evaluate *Bacillus* activity in plant-based and dairy matrices. This approach enhances our understanding of microbial physiology in complex food systems and provides a foundation for developing targeted strategies to improve food safety, stability, and product design.

Keywords: *Bacillus cereus*, *Bacillus subtilis*, isothermal calorimetry, microbial metabolism, cereulide, food matrix, plant-based food, metabolomics

1. Introduction

Microbial contamination is a key concern in the food industry (Snyder et al., 2024). In 2023, the United Nations estimated that 19% of all food available at the consumer level was wasted, which has a significant impact on the economy, environment, and public health (UNEP, 2024). The Gram-positive, spore-forming, facultative aerobe *Bacillus* spp. are ubiquitous in nature and include species such as *B. cereus* and *B. subtilis*. *Bacillus* species are usually introduced into the food production system through raw ingredients (Ehling-Schulz et al., 2015). *B. cereus* and *B. subtilis* both produce highly resistant spores, complicating their control with conventional techniques like heat, acid, and cleaning practices (Earl et al., 2008; Rahnama et al., 2023).

Bacillus cereus is an important foodborne pathogen, capable of causing diarrhoea due to enterotoxins or inducing vomiting due to the pre-formed heat- and acid-stable emetic toxin, cereulide (Ehling-Schulz et al., 2004). The *B. cereus* group, also known as *B. cereus sensu lato* (hereafter referred to as *B. cereus*), contains many genetically closely related species, including *B. cereus, B. mycoides,* and *B. thuringiensis*. *B. cereus* taxonomy has undergone many changes over the years, especially after the introduction of genome sequencing, and numerous nomenclatural frameworks have been used to describe *B. cereus* taxonomy (Carroll et al., 2022).

Foodborne disease caused by *B. cereus* is believed to be grossly underreported. Nevertheless, in 2022, *B. cereus* toxins (both emetic and enterotoxins) caused 306 registered foodborne outbreaks, 3192 cases of illness, 66 hospitalizations, and 2 deaths in the EU and UK alone (EFSA, 2023). *B. cereus* is typically isolated from plant materials (Messelhäusser et al., 2014), and given the increasing development of plant-based ingredients for food production (Kyrylenko et al., 2023). There is a strong need to monitor the prevalence and toxicity of *B. cereus* in plant matrices.

B. subtilis is a key driver of many traditional fermentations based on legumes, seeds, and tubers (Li et al., 2023). A high occurrence of *B. cereus* has been observed in *B. subtilis*-fermented food products, and its presence poses a significant concern for food safety (Owusu-Kwarteng et al., 2022). *B. subtilis* is also associated as a spoilage agent in foods, such as slime formation in rice products and ropiness in bread (Dong et al., 2023; Valerio et al., 2008). Consequently, understanding the metabolic characteristics, growth dynamics, and responses of *B. cereus* and *B. subtilis* is essential for assessing food safety and quality risks, particularly for plant-based food products.

An attractive tool for fast detection of microbial activity is isothermal microcalorimetry (IMC). IMC is a non-invasive method based on real-time, accurate measurements of heat flow generated by the metabolic activity of biological systems, especially in opaque or complex matrices where optical methods are limited. IMC equipment has become less costly and has demonstrated improved sensitivity

and accuracy (Braissant et al., 2010). IMC has recently been successfully applied to improve bacterial detection time in a clinical context (Cichos et al., 2023) and to investigate the metabolic activity of bacteria living in biofilms (Lichtenberg et al., 2022). Despite its potential relevance in non-invasive risk assessment of food, IMC has not yet been explored as a tool for monitoring the growth of pathogenic and non-pathogenic *Bacillus spp*.

While IMC provides valuable insights into the overall metabolic activity of microorganisms, it offers limited specificity regarding the biochemical processes underlying bacterial metabolism. Monitoring changes in key metabolites such as sugars, organic acids, and amino acids enables a deeper understanding of microbial nutrient assimilation while also revealing biochemical changes in the food matrices that are relevant to safety and quality. Sugars serve as primary energy sources for microbial growth, while organic acids are key intermediates in carbon metabolism (Schilling et al., 2007). Free amino acids are an important nitrogen source and can be released either through proteolytic activity or produced through de novo synthesis (Sonenshein, 2007). Furthermore, quantifying the heat-stable emetic toxin cereulide is essential for evaluating the safety risks associated with food products contaminated by *B. cereus*.

To advance understanding of *Bacillus* physiology in food systems, this study integrates isothermal microcalorimetry (IMC) with targeted metabolomic profiling. We investigate the metabolic heat production of *B. cereus* and *B. subtilis* in a rich laboratory medium and in dairy- and plant-based matrices, while quantifying key metabolites—sugars, organic acids, free amino acids, and cereulide—at selected time points. This combined approach offers a more nuanced view of microbial activity and its implications for food safety and quality.

2. Materials and methods

2.1 Bacterial strains

Sixteen strains from the *B. cereus* group and eight *B. subtilis* strains were selected based on diversity in toxicity, genetic characteristics, and origin (Table 1). Five of the included *B. subtilis* strains were previously isolated from traditional fermentations in Ghana and Burkina Faso (Kpikpi et al., 2014) (Parkouda et al., 2010; Wiedenbein et al., 2023). Two of the *B. cereus* strains were isolated from African fermented condiments (Thorsen et al., 2010). Strains were maintained in a -80°C glycerol stock and streaked onto Brain Heart Infusion (BHI) agar plates before being cultured in BHI broth.

100 TABLE 1: Characteristics of the *Bacillus* strains used in this study, based on sequencing and ANIm data for the *Bacillus cereus* group obtained by Skriver et
101 al. (2025) and for the *Bacillus subtilis* strains obtained by Wiedenbein et al. (2023). Asterisk (*) denotes values below species threshold (<96% ANIm). The
102 letter T refers to the type strain.

Strain	**Toxin production**	**Origin isolation**	**Previously assigned taxonomy (ANIm in %)**	**Taxonomy reference**	**Best taxonomic match (ANIm in %)**	**Assembly size (basepairs)**	**GC content**
F4433/73	Enterotoxin	Meatloaf, USA	*Bacillus cereus* (91.68*)	(Midura et al., 1970)	*Bacillus tropicus* (96.26)	5,433,211	35.5
O-216	Unknown	Milk, Denmark	*Bacillus cereus* (91.89*)	(Larsen & Jørgensen, 1999)	*Bacillus pacificus* (99.94)	5,655,403	35.4
LWL3	Enterotoxin	Foodborne outbreak	*Bacillus cereus* (91.68*)	(Dufrenne et al., 1995)	*Bacillus wiedmannii* (96.43), *Bacillus pretiosus* (97.1%)	5,686,534	35.3
59	Unknown	Cream	*Bacillus cereus* (91.72*)	(Stenfors & Granum, 2001)	*Bacillus wiedmannii* (96.56), *Bacillus pretiosus* (96.7%)	5,516,290	35.5
MC67	Emetic	Sandy soil, Denmark	*Bacillus weihenstephanensis*[a] (95*)	(Hendriksen et al., 2006)	*Bacillus mycoides* (95*)	5,802,073	35.5
A536	Enterotoxin	Milk, silotank	*Bacillus cereus* (89.96*)	(Svensson et al., 2004)	*Bacillus mycoides* (97.23)	6,122,672	35.3
NVH 0075-95	Enterotoxin	Foodborne outbreak in Norway	*Bacillus cereus* (92.08*)	(T. Lund & Granum, 1996)	*Bacillus paranthracis* (97.61)	6,044,751	35.3
F4810/72	Emetic	Foodborne outbreak, UK	*Bacillus cereus* (92.09*)	(Turnbull et al., 1979)	*Bacillus paranthracis* (97.62)	5,584,855	35.5
NS117	Emetic	Spruce tree, Norway	*Bacillus cereus* (92.04*)	(Hallaksella et al., 1991)	*Bacillus paranthracis* (97.61)	5,832,990	35.3
LKT1/1	Emetic	Filler material of a building with moisture damage, Finland	*Bacillus cereus* (92.06*)	(Apetroaie et al., 2005)	*Bacillus paranthracis* (97.62)	5,690,232	35.5
Y48H10	Emetic	Iru, Africa	*Bacillus cereus* (92.09*)	(Thorsen et al., 2010)	*Bacillus paranthracis* (97.62)	5,549,004	35.5

Ba18H2	Emetic	Sonru, Africa	*Bacillus cereus* (92.09*)	(Thorsen et al., 2010)	*Bacillus paranthracis* (97.62)	5,598,436	35.5
SDA GR177	Emetic + Enterotoxin	Milk	*Bacillus cereus* (92.09*)	Svensk Mjolk, Swedish Dairy Association	*Bacillus paranthracis* (97.62)	5,634,738	35.5
SDA MA60	Enterotoxin	Milk	*Bacillus cereus* (92.06*)	Svensk Mjolk, Swedish Dairy Association	*Bacillus paranthracis* (97.62)	5,644,507	35.5
F4430/73	Emetic	Foodborne outbreak, UK	*Bacillus cereus* (92.06*)	(Spira & Goepfert, 1975)	*Bacillus paranthracis* (97.62)	5,661,860	35.5
ISI2489	Emetic	Unknown	*Bacillus cereus* (92.08*)	Arla culture collection	*Bacillus paranthracis* (97.64)	5,541,441	35.5
DSM13019		Boiled hay, Denmark	*Bacillus subtilis* (98.53)	(Wiedenbein et al., 2023)	*Bacillus subtilis* (98.53)	4,044,377	43.6
DSM10 T		Unknown ("Marburg")	*Bacillus subtilis* (99.99)	(Lilge et al., 2021; Wiedenbein et al., 2023)	*Bacillus subtilis* (99.99)	4,299,854	43.4
DSM21393		potato tubers, Tatarstan, Russian Federation	*Bacillus subtilis* (98.8)	(Wiedenbein et al., 2023)	*Bacillus subtilis* (98.8)	4,100,908	43.9
PRO35		Kantong, Nyankpala, Ghana	*Bacillus subtilis* (98.4)	(Kpikpi et al., 2014; Wiedenbein et al., 2023)	*Bacillus subtilis* (98.4)	4,032,381	43.4
PRO31		Kantong, Nyankpala, Ghana	*Bacillus subtilis* (98.35)	(Kpikpi et al., 2014; Wiedenbein et al., 2023)	*Bacillus subtilis* (98.35)	4,272,877	43.2
PRO64		Kantong, Nyankpala, Ghana	*Bacillus subtilis* (97.9)	(Wiedenbein et al., 2023)	*Bacillus subtilis* (97.9)	4,113,761	43.6
PRO99		Kantong, Navrongo, Ghana	*Bacillus subtilis* (98.2)	(Wiedenbein et al., 2023)	*Bacillus subtilis* (98.2)	3,963,991	43.4
PRO115		Maari, Mansila, Burkina Faso	*Bacillus subtilis* (100)	(Wiedenbein et al., 2023)	*Bacillus subtilis* (100)	4,140,503	43.8

Footnote *(a): B. mycoides* has been used for ANIm comparison, as *B. mycoides* is a later synonym of *B. weihenstephanensis* (Liu et al., 2018).

104 **2.2 Whole genome sequencing**

105 *Bacillus subtilis* whole genomes included in this work were previously characterized in Wiedenbein et
106 al. (2023), while the *Bacillus cereus* whole genomes were obtained from Skriver et al. (2025).

107 **2.3 Phylogenetic tree construction**

108 Phylogenetic trees were constructed with the up-to-date bacterial core gene (UBCG) method based on
109 the concatenation of 92 core genes found in all taxonomic ranks of Bacteria (Na et al., 2018). FastTree
110 was selected to generate the maximum-likelihood phylogenetic trees (Price et al., 2010). The
111 phylogenetic trees were visualized with Molecular Evolutionary Genetics Analysis version 11 software
112 (MEGA 11) (Tamura et al., 2021). *Halobacillus halophilus* DSM 2266 (type strain) (GenBank:
113 GCA_000284515.1) was selected as the outgroup to root the trees.
114

115 **2.4 Isothermal calorimetric assessment of *B. cereus* and *B. subtilis* in BHI medium**

116 All sixteen *B. cereus* and eight *B. subtilis* strains (Table 1) were cultivated in BHI broth (Merck). To
117 measure the heat flow of the *Bacillus* strains in BHI medium, the protocol of Beilharz et al. (2023) was
118 followed with a few modifications. Strains were cultured in BHI broth overnight (30°C, 200 rpm) and
119 then diluted with BHI broth to an optical density at 600 nm (OD600) of 0.2. The inoculum was mixed
120 with fresh BHI medium, with an inoculation rate of 1% and a total volume of 200 µL. The inoculated
121 mixtures were transferred to plastic inserts (calWells™, Symcel AB, Sweden) in the titanium vials of a
122 48-well calPlate™ (Symcel AB, Sweden). The vials were pre-incubated for 60 min to reach temperature
123 equilibrium. The plates were then incubated in the Calscreener (Symcel AB, Sweden) at 30°C for 20h.
124

125 **2.5 Isothermal calorimetric assessment of *B. cereus* and *B. subtilis* in food matrices**

126 Oat drinks (Naturli, Denmark) and UHT whole milk (Geia Food A/S, Czech Republic) were purchased
127 commercially in Danish supermarkets. For the mixed oat-pea matrix, 5% w/w pea protein hydrolysate
128 (NUTRALYS® PEA F853M-EXP, Roquette, France) was transferred to store-bought oat drink and
129 autoclaved (121°C, 20 min). For the pea matrix, 5% w/w was added to MilliQ water and autoclaved
130 (121°C, 20 min). A selection of three *B. cereus* strains (Y48H10, SDA GR177, MC67) and three *B.*
131 *subtilis* strains (PRO99, DSM10, DSM21393) were cultivated in the food matrices.

132 Cells were cultured in BHI broth overnight (30°C, 200 rpm), centrifuged at 4500 *g* for 12 minutes, and
133 washed twice in 0.9% NaCl solution. Washed cells were adjusted to OD600 of 0.2 before being
134 transferred with an inoculation rate of 1% and a total volume of 200 µL into the different food matrices.
135 Similarly to section 2.5, the inoculated mixtures were transferred to plastic inserts in the titanium vials

136 of the 48-well calPlate and pre-incubated for 60 min to reach temperature equilibrium. The calPlate was
137 then incubated in the Calscreener at 30°C for 24 hours.

138 **2.6 Cultivation in oat, pea, and oat-pea matrices for metabolic profiling**

139 One strain from each species (*B. cereus* Y48H10 and *B. subtilis* DSM21393) was selected for in-depth
140 metabolic profiling. Washed cells were prepared as in section 2.5 and then inoculated in oat, pea, and
141 oat-pea matrices. For this experiment, two biological replicates, each consisting of four technical
142 replicates, were used. Biological replicates were defined as individual colonies streaked from the same
143 BHI plate, while technical replicates originated from the same biological replicate after two rounds of
144 pre-cultivation on BHI broth. Samples were taken at maximum calorimetric growth rate, approximately
145 8 hours for *B. cereus* and 11 hours for *B. subtilis*, and at the end-metabolic point, 24 hours for both *B.*
146 *cereus* and *B. subtilis*. Directly after sampling, technical replicates were pooled to obtain a final volume
147 of approximately 800 µL. This pooled sample was analysed for sugars and organic acids (sections 2.7),
148 free amino acids (section 2.8), and the *B. cereus* samples also for cereulide (section 2.9).

149 **2.7 Quantification of simple sugars and organic acids produced by HPLC-RID**

150 Pooled technical replicates of food samples were centrifuged at 12000 *g* for 15 minutes, and the
151 supernatant was separated and filtered through PTFE membranes with a pore size of 0.45 µm directly
152 into the HPLC vials and stored at -21°C until analysis.

153 An Agilent 1260 Infinity II LC system with refractive index detection (Agilent Technologies, Santa
154 Clara, CA, U.S.A.) was used to quantify simple sugars and organic acids at 35°C. The mobile phase
155 was water, with a flow rate of 0.5 mL/min. A Cation H Bio-Rad Micro-Guard column (304.6 mm)
156 followed by an Aminex HPX-87H carbohydrate analysis column (300 × 7.8 mm) (Bio-Rad
157 Laboratories, Inc.; Hercules, CA, U.S.A.) was used to separate organic acids and simple sugars
158 isocratically at 35°C. The injection volume of the sample was 10 µL and the run time was 15 minutes.

159 The chromatographic data were acquired, monitored, and processed using OpenLAB CDS LC
160 Chemstation M8307AA. Quantification and assignment of peaks were based on the peak areas and
161 retention times of known standard curves for purified external calibration curves prepared using seven
162 standard solutions for sugars (glucose, fructose, arabinose, galactose, and sucrose) and organic acids
163 (lactic-, acetic-, and citric acid) in concentrations ranging from 0.05 – 10 g/L.

164 **2.8 Free Amino Acid analysis**

165 Samples were freeze-dried (Lyovapor L-200, Buchi) for two days. To each freeze-dried sample, 1 mL
166 of 0.1 M HCl was added, and the mixture was ultrasonicated (Branson 2210, Emerson) for five minutes.
167 To the 200 µL sonicated sample, 200 µL of an ice-cold solution of 12.5% trichloroacetic acid was added.

After incubation for 2 hours at 4°C, the sample was centrifuged at 10,000 g for 20 minutes. The supernatant was neutralized with 45 µL of freshly prepared 1 M NaOH and then mixed with 195 µL of 50 µM aminocaproic acid (internal standard). Free amino acids were quantified using HPLC, with mobile phase compositions and HPLC settings as in Rehlund et al. (2025). All standard free amino acids were quantified, except cysteine and proline. HPLC data were pre-processed using Chromeleon 7.2.7 (Thermo Scientific, MA, USA).

2.9 Quantification of cereulide produced by strain Y48H10 using HPLC-MS/MS

Quantification of cereulide from strain Y48H10 was performed in two biological duplicates. Four technical replicates were pooled together for each sampling time point. Cereulide analysis was performed using ISO 18465 standard (Anonymous, 2017) method with few modifications. Briefly, samples were diluted in 1:10 ratio with HPLC-grade acetonitrile (VWR Chemicals, Poland). Labelled cereulide (^{13}C6-cereulide) was added as an internal standard in each sample at the concentration of 10 ng/ml. The cereulide was extracted by a rotating shaker (300 rpm) for 1 hour followed by resting for 30 minutes. The solution was decanted twice (first 4500 rcf for 15 minutes and second 12,000 rcf for 15 minutes). A 200 µL of the supernatant was transferred into HPLC vial for LC-MS/MS analysis.

Samples were randomized and analysed on an Elute UPLC system coupled to an Impact II QTOF-MS instrument (Bruker Daltonik, Germany). Chromatographic separation was performed on a reverse-phase Supelco Discovery C18 column (10 cm × 2.1 mm, 5 µm particle size) maintained at 36 °C. The mobile phase consisted of an isocratic elution with 5% phase A (10 mM ammonium formate in water containing 0.1% formic acid) and 95% phase B (acetonitrile with 0.1% formic acid). The flow rate was set to 0.4 mL/min with an injection volume of 5 µL. Mass spectra were acquired in the range of m/z 1000–1300 at 12 Hz using electrospray ionization (ESI) in positive-ion mode. Prior to analysis, the instrument was externally calibrated with 10 mM sodium formate in 50% isopropanol and tuned using the ESI-L Low Concentration Tuning Mix (Agilent Technologies, CA, USA). ESI parameters were as follows: end plate offset, –500 V; capillary voltage, 4500 V; nebulizer pressure, 2.2 bar; dry gas flow, 10 L/min; and drying temperature, 220 °C. MS settings included funnel 1 and 2 RF, 200 Vpp; hexapole, 50 Vpp; ion energy, 5 eV; collision energy, 5 eV; and pre-pulse storage, 5 µs. Peak areas of natural cereulide and isotope-labelled cereulide were extracted using ion traces corresponding to their precursor ions at m/z 1170–1171 and 1176–1177, respectively.

2.10 Data analysis

Isothermal microcalorimetric data were analysed from 1 to 24 hours after inoculation, as the first hour was needed for thermal equilibration of the instrument. Baseline correction was applied using the heat flow data collected before plate insertion. For 2 out of 96 experiments, an alternative baseline heat flow value was selected to achieve a better fit after plate insertion at 50 minutes. Data from one replicate

experiment corresponding to strain *B. subtilis* PRO31 was excluded, due to negative heat flow values at the beginning of the experiment, which was attributed by the instrument manufacturer to moisture evaporation from the vial.

The heat curves (heat accumulated as a function of time) were fitted with the Gompertz model to estimate microbial growth characteristics (Zwietering et al., 1990), based on two assumptions (1) that cells remain in the medium, and (2) that heat flow data present themselves with one central peak or a closely similar shape (e.g. peak with a shoulder) (Braissant et al., 2010). Data analysis of the isothermal calorimetry was conducted using RStudio (R Core Team, 2023). Curve fitting and parameter estimation were performed on each experiment using the grofit R package, based on Gompertz modelling, to estimate the maximum heat production (mJ), the length of the calorimetric lag time (h), and the maximum calorimetric growth rate ($mW \cdot h^{-1}$) (Kahm et al., 2010). The lag time was corrected for the one-hour pre-incubation period. Statistical tests were performed using the Gompertz parameters related to species, with a significance level of 0.05. Group comparisons between *B. cereus* and *B. subtilis* and between the interspecies clades in BHI medium were performed using unpaired T-tests, and phylogenetic comparisons between *B. cereus* clades were performed using Kruskal-Wallis with Dunn's post-hoc test. Comparison between heat curves obtained in BHI media and food matrices of selected *B. cereus* (Y48H10, SDA GR177, MC67) and *B. subtilis* strains (PRO99, DSM10, DSM21393) were conducted using paired t-test with Bonferroni correction.

A two-way analysis of variance (ANOVA) was performed to examine the effects of *Bacillus* clade (*B. cereus* and *B. subtilis*), food (milk, oat, pea, and oat-pea), and their interaction on the square-root transformed Gompertz parameters. A separate two-way ANOVA was performed to test the influence of all matrices (foods and BHI medium), *Bacillus* clade, and their interaction on square-root transformed Gompertz parameters. All ANOVA models were fitted using the lmerTest package, which extends lme4 by providing p-values for mixed effects. Post-hoc analyses were conducted using estimated marginal means (EMM) via the emmeans package. For the metabolomics data, a three-way ANOVA was performed to evaluate the influence of *Bacillus* clade, metabolic time-point (peak vs. end), and food matrix, as well as their interactions, on the content of individual sugars, individual organic acids, and total free amino acids. Biological replicates were included as a random effect using lme4, and significance testing was carried out with lmerTest. Post-hoc analyses were conducted using EMM. Additionally, a two-way ANOVA was conducted to investigate the effects of fermentation (non-fermented vs. fermented) and matrix on total sugars. Tukey post-hoc comparisons were performed between non-fermented and fermented samples within each matrix (oat, pea, and oat–pea). Non-detected compounds were assigned a value equal to half the lowest detected concentration to enable statistical comparisons. Principal component analysis (PCA) was applied to investigate potential

236 interactions between the metabolites of *Bacillus* spp. in food matrices using RStudio (R Core Team,
237 2023), and a biplot was created using the ggplot2 package.

238 The quantification of cereulide produced by *B. cereus* strain Y48H10 in food matrices was based on
239 mass spectrometric peak area ratios derived from baseline-corrected chromatograms, using a signal-to-
240 noise ratio (SNR) threshold of 3. The limit of detection (LOD) and limit of quantification (LOQ) were
241 determined from the standard deviation of the noise in 0.1 ng/mL samples, which represented the lowest
242 concentration at which cereulide was not detectable. Inspection and processing of obtained cereulide
243 data were performed using MATLAB 2023b.

244 3. Results

245 3.1 Taxonomy and phylogeny

246 A maximum-likelihood phylogenetic tree was constructed using the UBCG pipeline (Na et al., 2018)
247 from the whole-genome sequences of the *B. cereus* and *B. subtilis* strains. Species names were drawn
248 from the best taxonomic (ANIm) matches rather than the previously recognized taxonomy of the strains
249 (Table 1). For strains BC59 and LWL3, previously classified as *B.* cereus, ANIm values exceeded the
250 species threshold (>96%) for both *Bacillus wiedmannii* and *Bacillus pretiosus*. However, we adopted
251 *B. wiedmannii* as the taxonomic designation, in line with (Mozhaitseva et al., 2025), who reported
252 genomic similarity between these species and grouped them within a shared cluster. Moreover, *B.*
253 *pretiosus* remains an effectively published but not validly recognized name under current bacterial
254 nomenclature rules (Oren et al., 2023; Robas Mora et al., 2023), further supporting the use of *B.*
255 *wiedmannii*. Five different clades were identified (Figure 1), differentiating the *B. cereus* group strains
256 into (Clade A) *B. paranthracis, B. pacificus,* and *B. tropicus*, (Clade B) *B. wiedmannii/B. pretiosus*, and
257 (Clade C) *B. mycoides*, and distinguishing the *B. subtilis* group into (Clade D) PRO31, PRO35, PRO64,
258 PRO99, and (Clade E) DSM13019, DSM21393, PRO115, and DSM10. In short, we observed a diverse
259 range of *B. cereus* (encompassing five different genomic subspecies) and *B. subtilis* isolates (two
260 distinct clades) to facilitate comparisons between phylogeny and microcalorimetric analysis of
261 metabolic activity.

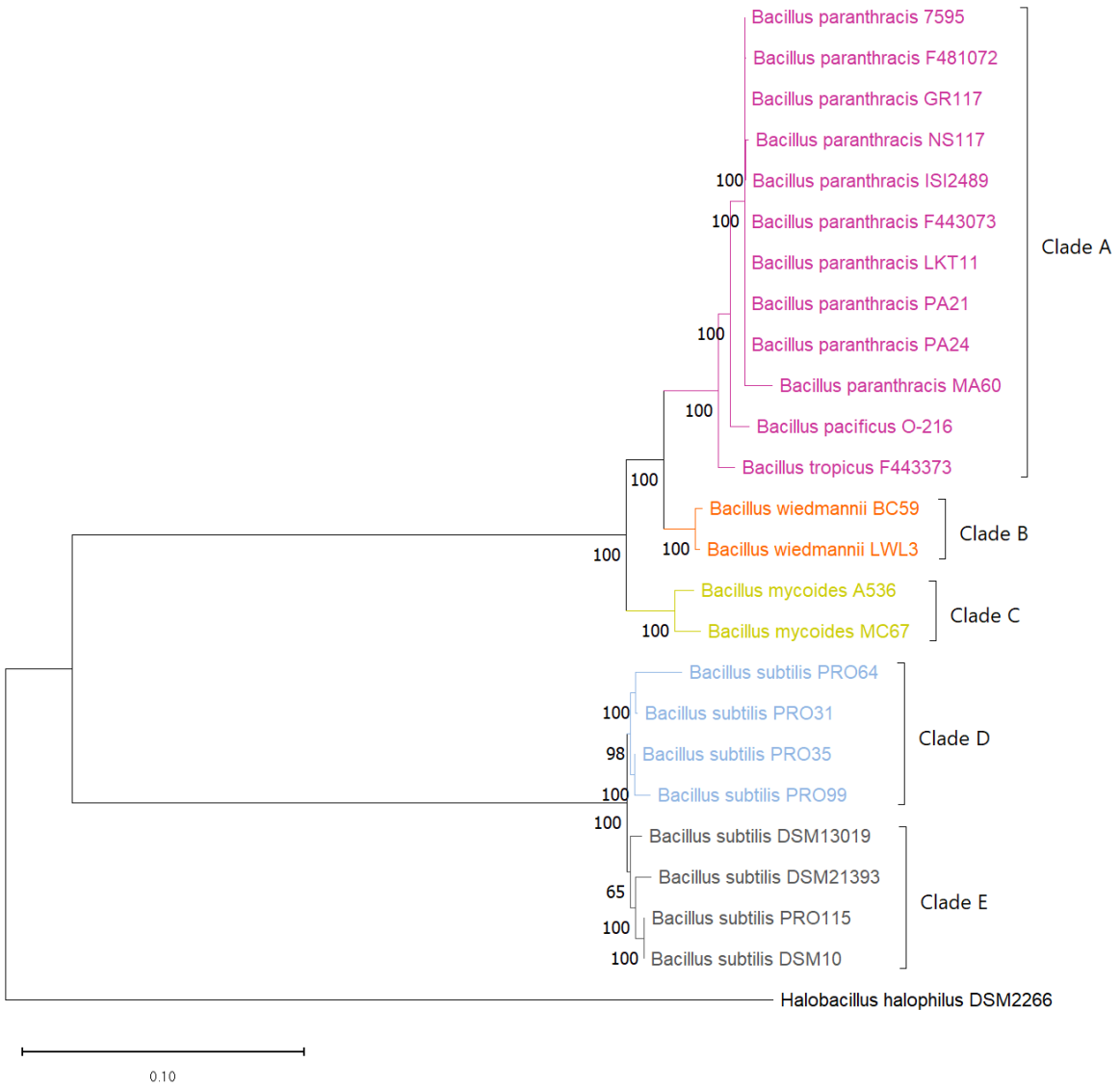

Figure 1: Rooted maximum likelihood phylogenetic tree of Bacillus cereus *group strains (Clades A, B, and C) and Bacillus subtilis strains (Clades D and E) using the up-to-date bacterial core gene (UBCG) pipeline, drawn by MEGA11. The names of the species were drawn from the best taxonomic (ANIm) matches, as displayed in Table 1.* Halobacillus halophilus *DSM2266 was used to root the tree. Percentage bootstrap values are indicated at branching points, and the scale bar represents 0.01 substitutions per site.*

3.2 Metabolic activity of *Bacillus* cultivated in BHI and food matrices

To investigate the metabolic activity of *Bacillus* strains under controlled conditions, we monitored the metabolic heat production profiles of 16 *B. cereus* strains and 8 *B. subtilis* strains. Cultivation was first carried out in BHI medium at 30°C for 20 hours, until the metabolic activity reached a steady-state plateau (Figure 2B). During 20 hours of cultivation, *B. cereus* and *B. subtilis* exhibited a typical

274 sigmoidal pattern in the heat production curves (Figure 2A). The heat flow profiles of both *B. subtilis*
275 and *B. cereus* exhibit one main peak followed by a second shoulder peak (Figure 2B).

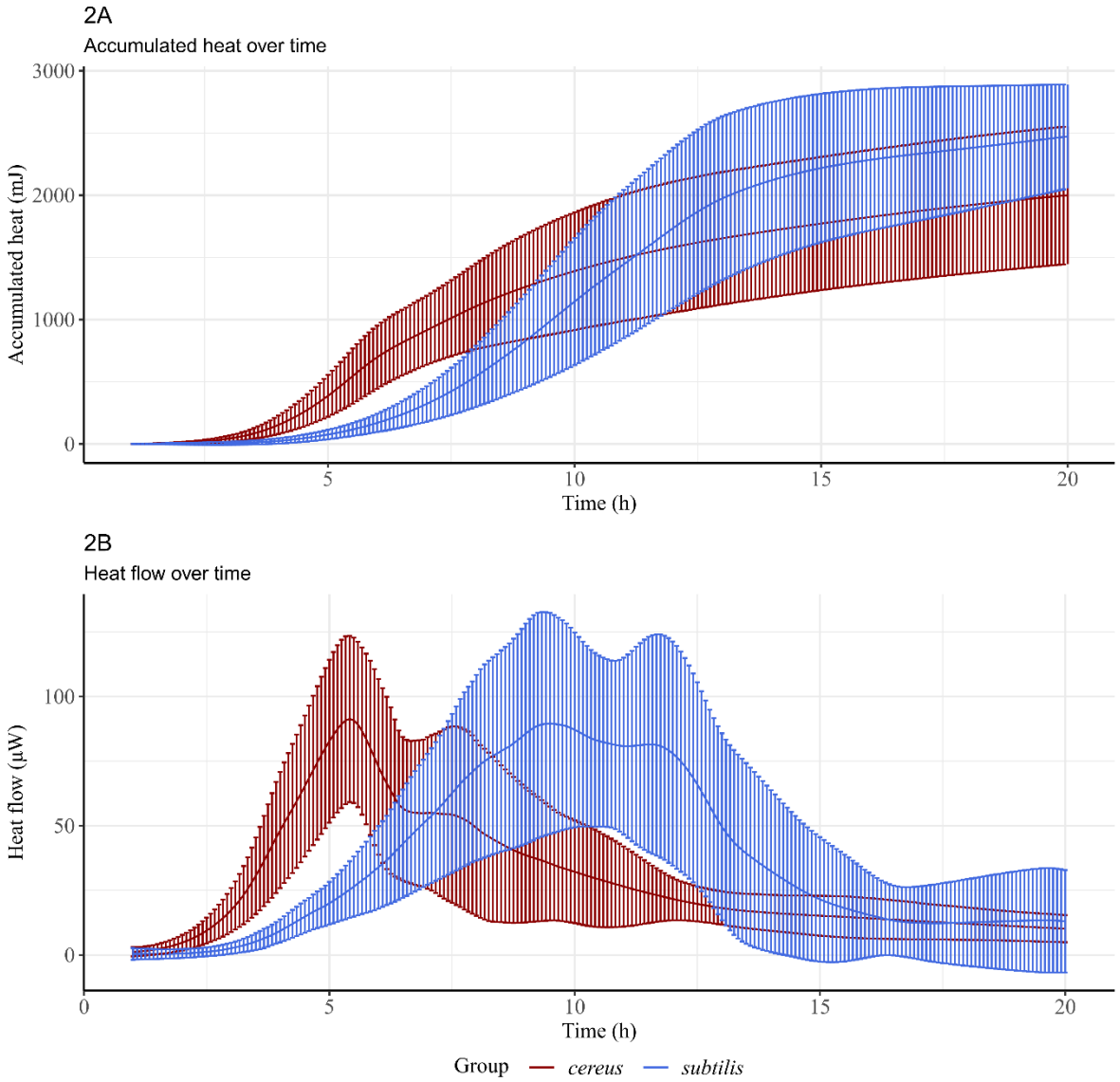

276

277 *Figure 2*: *Metabolic heat characteristics of 16* B. cereus *(red) and 8* B. subtilis *(blue) strains cultivated*
278 *in BHI medium, based on four biological replicates divided between two different experiments (2A)*
279 *Mean values (curve) and standard deviation (error bars) of accumulated heat production over time*
280 *(2B) Mean values (curve) and standard deviation (error bars) of heat flow over time of 16* B. cereus
281 *(red) and 8* B. subtilis *(blue) strains.*

282 To gain a better understanding of the metabolic heat profiles, fitted parameters from the Gompertz
283 model, lag time (h), the maximum calorimetric growth rate ($mJ*h^{-1}$), and total heat (mJ), were plotted
284 for each *Bacillus* group (*cereus* vs. *subtilis*) (Figure 3A) and the phylogenetic clades within *B. cereus*
285 and *B. subtilis* groups (A, B vs. C; D vs. E) (Figure 3B). Between the *B. subtilis* and *B. cereus* groups,
286 significant differences were observed across all parameters. *B. subtilis* released a significantly higher

287 amount of total heat (2732 mJ ± 462) than *B. cereus* (1941 mJ ± 566) ($p < 10^{-10}$). *B. subtilis* displayed
288 a higher maximum metabolic activity (378 h^{-1} ± 140) than *B. cereus* (240 h^{-1} ± 106) ($p < 10^{-5}$). Finally,
289 a longer lag time was observed for *B. subtilis* (7.9 hours ± 1.0) than for *B. cereus* (4.3 hours ± 0.8) ($p <$
290 10^{-16}).

291 In addition, differences in metabolic activity were observed within the *B. subtilis* and *B. cereus* groups.
292 Between the *B. cereus* clades, *B. mycoides* strains from clade C produced a significantly lower amount
293 of total heat (971 mJ ± 292) than *B. paranthracis*, *B. pacificus,* and *B. tropicus* strains from clade A
294 (2119 mJ ± 464, $p <10^{-5}$) and *B. wiedmannii* strains from clade B (1839mJ ± 212, p = 0.01). In addition,
295 the maximum calorimetric growth rate differed significantly between Clade A and B ($p <10^{-5}$) and
296 between Clade A and C (p <10-5). Between the *B. subtilis* clades, clade D strains exhibited a longer lag
297 time (8.6 hours ± 0.8) than Clade E (7.2 hours ± 0.7) ($p <10^{-5}$).

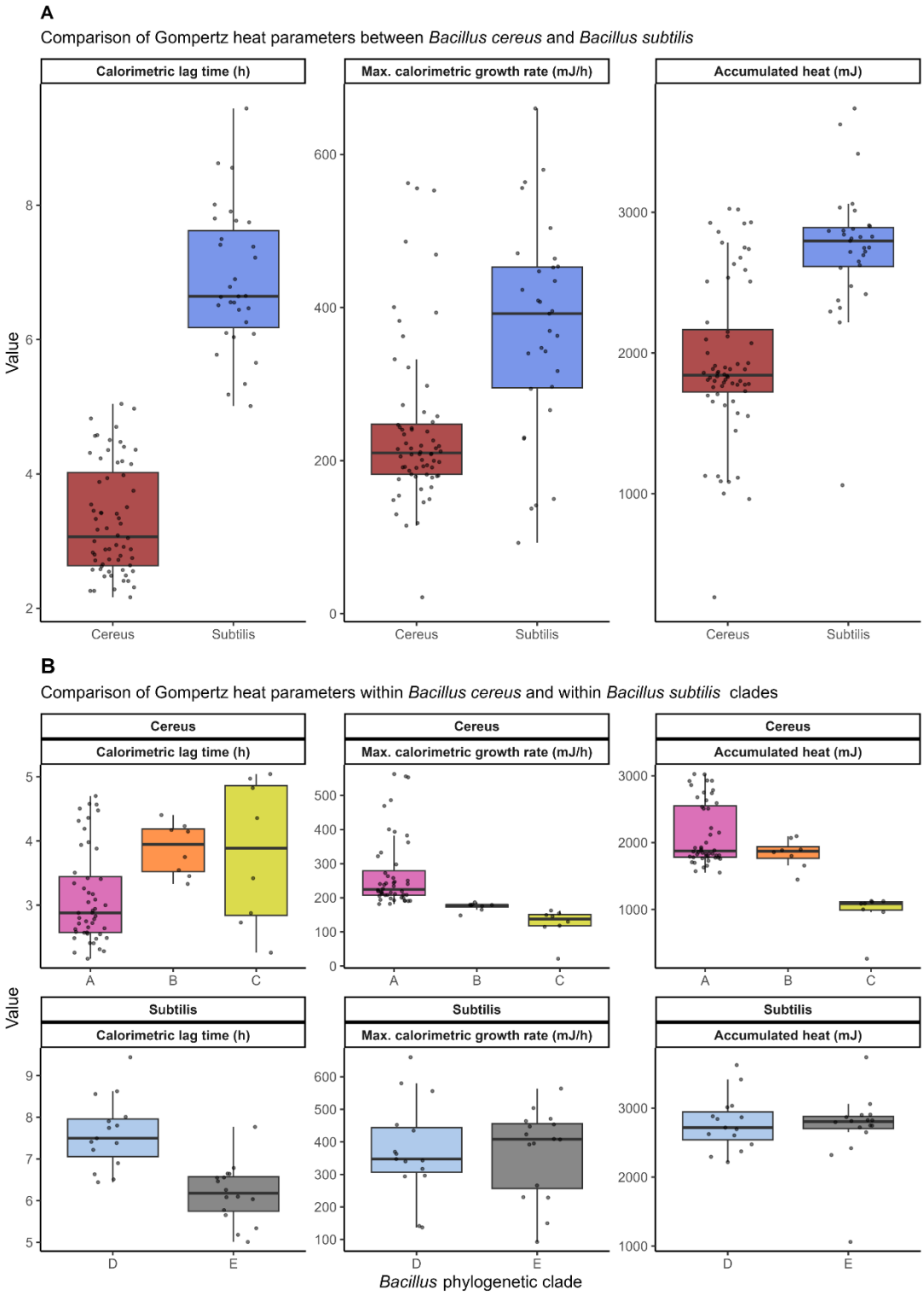

298

299 *Figure 3: Differences in heat flow characteristics, including calorimetric lag time (h), maximum*
300 *calorimetric growth rate (mJ*h^{-1}), and total heat (mJ). Calorimetric lag time was corrected for 1 h*
301 *pre-incubation period. (3A): Differences in heat flow characteristics between the subtilis and cereus*
302 *groups. (3B): Differences in heat flow characteristics between the phylogenetic clades as defined in*
303 *Figure 1, between Clade A (*B. paranthracis, B. pacificus *and* B. tropicus*), B (*B. wiedmannii*), C (*B.
304 mycoides*), D (*B. subtilis *PRO31, PRO35, PRO64, PRO99) and E (*B. subtilis *DSM13019,*
305 *DSM21393, PRO115 and DSM10)*

306 In addition to BHI, four strains of *B. cereus* (Y48H10, SDA GR177, MC67) and three *B. subtilis*
307 (PRO99, DSM10, DSM21393) were cultured in food matrices (milk, oat, pea, and oat-pea) at 30°C.
308 Their metabolic heat activity was monitored for 24 hour periods. The pea and oat-pea matrices were
309 autoclaved prior to inoculation. In contrast, the oat was not autoclaved based on preliminary findings:
310 *B. cereus* did not metabolize autoclaved oat, but autoclaving was necessary to solubilize the pea
311 hydrolysate. Gompertz parameters were subsequently derived from the calorimetric data (Table 2).

312 Table 2: Gompertz calorimetric growth parameters (mean (± sd)) of *B. cereus* Y48H10 and *B. subtilis*
313 DSM21393 cultivation in milk, oat, pea, and oat-pea matrices.

Species	Food	Calorimetric lag time [hours]	Max calorimetric growth rate [mJ/h]	Max accumulated heat [mJ]
B. cereus	Milk	7.4 (± 0.5)	150 (± 8)	2040 (± 120)
	Oat	14.5 (±12.8)	184 (± 97)	1696 (± 865)
	Pea	7.7 (± 0.3)	216 (± 65)	1663 (± 714)
	Oat-pea	9.8 (±1.7)	407 (± 103)	1880 (± 665)
B. subtilis	Milk	12.4 (± 2.7)	109 (± 30)	2057 (± 334)
	Oat	11.6 (± 3.1)	211 (± 43)	2452 (± 212)
	Pea	10.4 (±1.3)	275 (± 40)	2065 (± 301)
	Oat-pea	10.9 (± 0.4)	419 (± 28)	2403 (± 232)

314 *B. subtilis* exhibited a more consistent calorimetric lag time across food matrices, with a longer lag time
315 in milk (12.4 hours ± 2.7) compared to *B. cereus* (7.35 hours ± 0.5). Maximum calorimetric growth
316 rates varied significantly by substrate and were higher in the combined oat-pea matrix compared to oat
317 ($p = 0.002$, EMM), pea ($p = 0.01$, EMM), and milk ($p < 10^{-4}$, EMM). Across all food matrices, *B. subtilis*
318 produced more metabolic heat than *B. cereus* ($p = 0.02$, EMM), consistent with observations on BHI
319 medium. When comparing *Bacillus* metabolism between BHI and the food matrices, the calorimetric
320 lag time was significantly lower in BHI than in oat ($p = 0.02$, EMM), while no significant differences
321 were observed between the other matrices.

322 **3.3 Metabolic profiling of *Bacillus* growth in oat, pea, and oat-pea matrices**

323 Targeted metabolomic profiling was performed to assess how matrix composition influences *Bacillus*
324 metabolic activity, with particular focus on the enhanced growth observed in the combined oat-pea
325 matrix. One *B. subtilis* (DSM21393) and one *B. cereus* strain (Y48H10) were selected for cultivation
326 on the food matrices and sampled at two time-points: at peak metabolic activity (8 hours for *B. cereus,*
327 11 hours for *B. subtilis*) and at minimum metabolic activity (24 hours for both).

Sugars, organic acids, and free amino acids were quantified in all samples. To interpret the multifactorial data generated from targeted metabolomic profiling (simple sugars, organic acids, and free amino acids), principal component analysis (PCA) was employed to visualize trends in metabolite synthesis and consumption by *B. subtilis* and *B. cereus* cultured in plant-based matrices over 24 hours. PCA revealed that matrix composition was the main driver of sample separation (Figure 4). PC1 (41% variance) was associated with free amino acids, galactose, and fructose. In comparison, PC2 (25% variance) separated the pea matrix from the oat and oat-pea, reflecting lower sugar levels (sucrose, glucose) and higher citrate content.

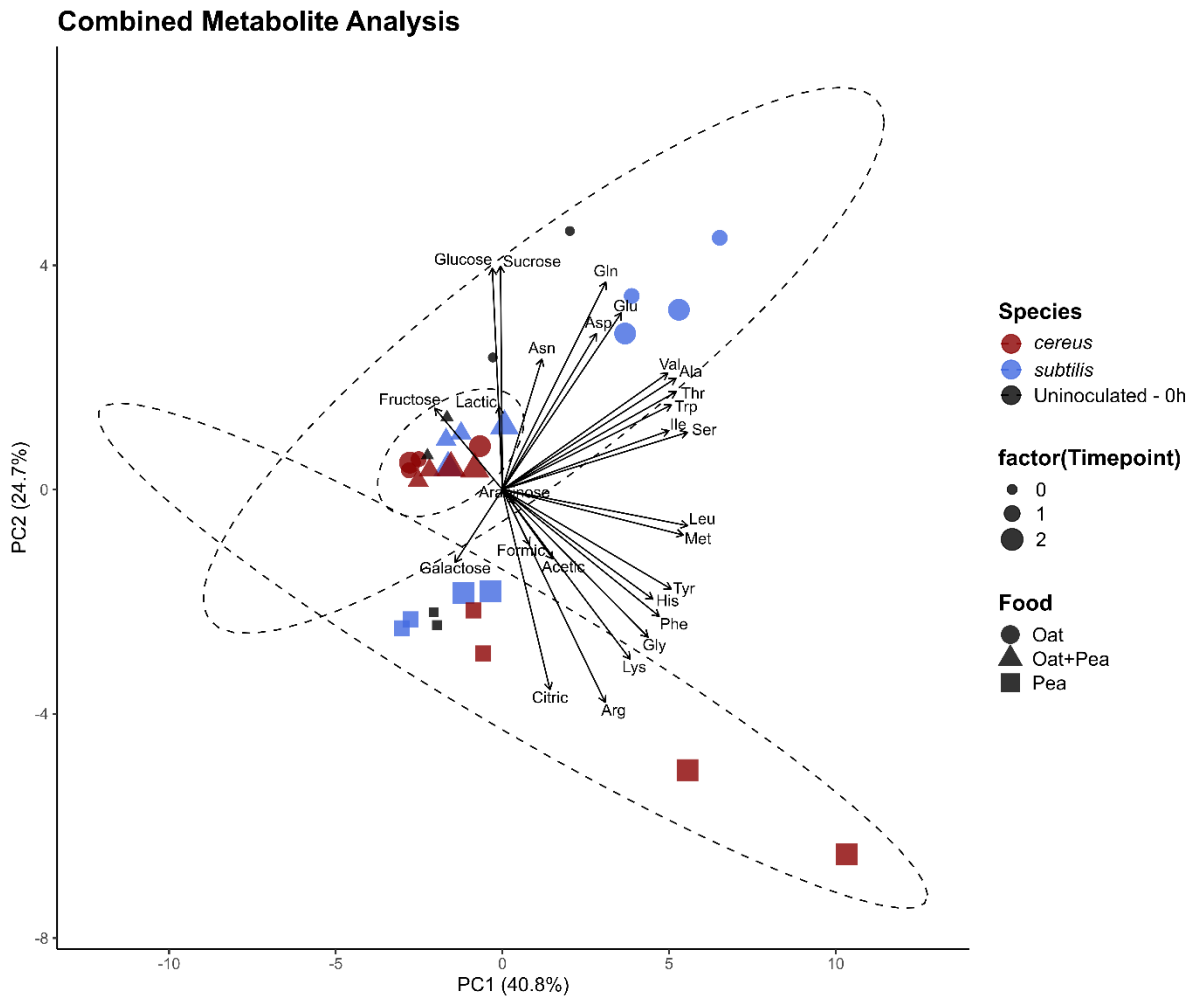

Figure 4: PCA biplot of Bacillus cereus *Y48H10 (red) and* Bacillus subtilis *DSM21393 (blue) metabolizing free amino acids, simple sugars, and organic acids in oat (circles), pea (squares), and oat-pea (triangles). Ellipses represent 95% of the population for each food matrix.*

To gain insight into the factors driving PCA separation, we analysed temporal changes in sugars, organic acids, and free amino acids. Matrix composition strongly influenced sugar and organic acid profiles. Total sugar content, as quantified by HPLC-RID, was significantly higher in the uninoculated oat (49.4 ± 1.8 g/L) and oat-pea (52.6 ± 3.6 g/L, $p = 0.001$, Tukey, Figure 5A) matrices compared to pea

344 (0.74 ± 0.00 g/L, p = 0.001, Tukey, Figure 5). *Bacillus* fermentation significantly reduced the total
345 amount of sugars in the oat-pea matrix (p = 0.01, two-way ANOVA, EMM). Citrate was uniquely
346 present in the pea matrix and absent from both oat and oat-pea (Figure 5B), contributing to its distinct
347 separation in PCA (Figure 4). Cultivation of *B. subtilis* and *B. cereus* led to an increase in total organic
348 acids from peak to end metabolic phase ($p = 10^{-5}$, three-way ANOVA). The oat-pea matrix showed the
349 most pronounced increase in organic acids, with both species sharply increasing lactic acid levels (p =
350 10^{-4}, EMM, Figure 5B). In contrast, the changes in organic acid levels in oat and pea were more modest
351 ($p > 0.05$, EMM). During *B. subtilis* growth on pea, citrate was consumed, and acetic acid was produced.
352 *B. cereus* produced more acetic acid than *B. subtilis* after 24 hours ($p = 10^{-4}$, EMM).

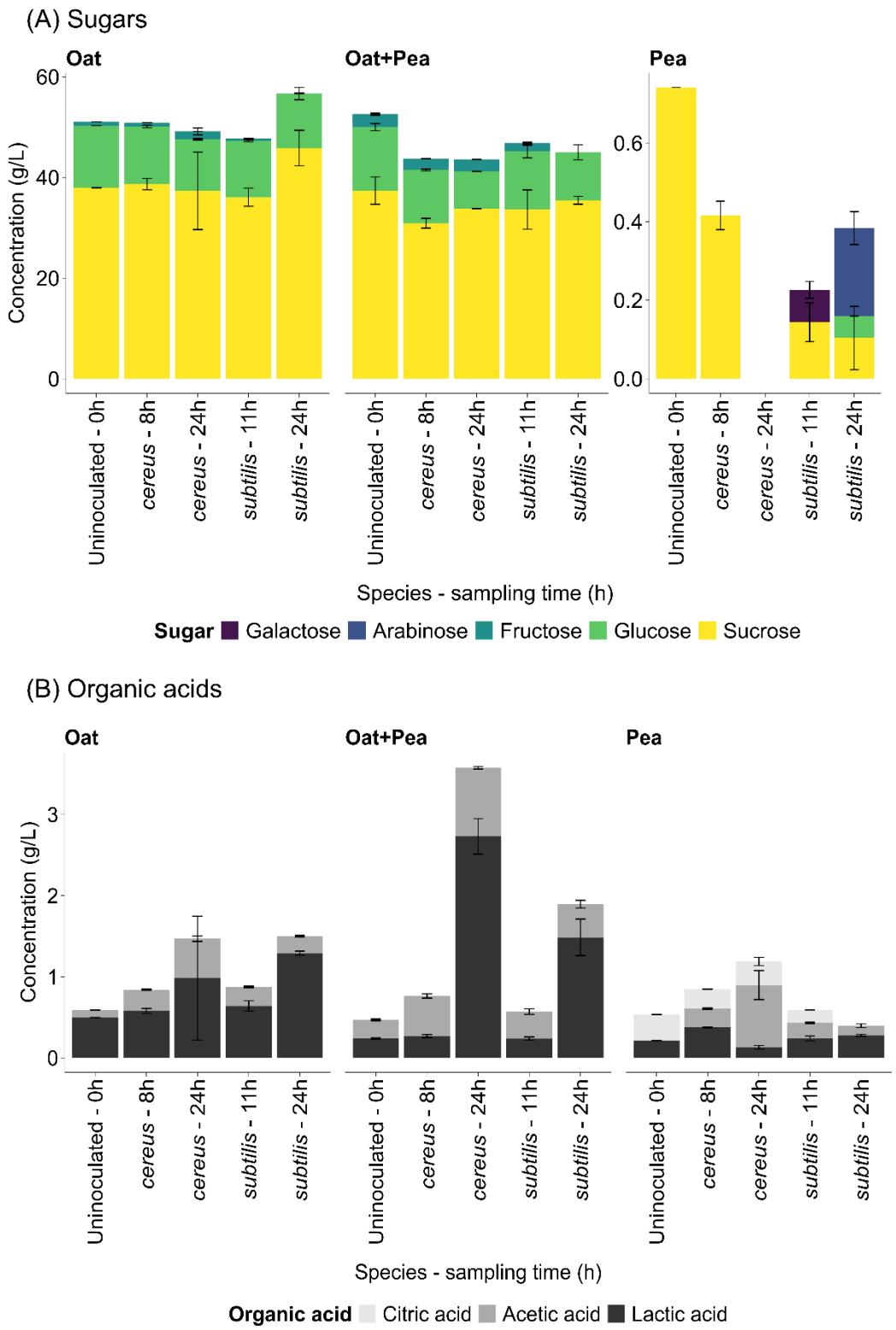

Figure 5: Metabolic profiling of Bacillus cereus *Y48H10 and* Bacillus subtilis *DSM21393 cultivated in oat, pea, and oat-pea matrices. Error bars are based on two biological replicates, each of which consists of four pooled technical replicates (A) sugar composition, (B) organic acid composition.*

Free amino acids were observed in all uninoculated matrices, with the highest levels detected in the (non-autoclaved) oat drink (Figure 6). *B. cereus* and *B. subtilis* had distinct effects on the free amino acid profiles depending on the matrix. The most pronounced effects were observed during *B. subtilis* growth on oat and *B. cereus* growth on pea, both increasing free amino acid levels, as also reflected in the PCA (Figure 4). These effects differed in the types of free amino acids released and the timing of their accumulation. For *B. cereus* in pea, total free amino acids increased from 59 µmol/g ± 1 (8 hours) to 219 µmol/g ± 54 (24 hours) ($p = 0.003$, EMM), primarily due to accumulation of Gly, Phe, Ala, Ser, Leu and Tyr. In contrast, *B. subtilis* displayed higher total free amino acid levels in oat than in pea ($p = 10^{-4}$, EMM), peaking at 227 µmol/g ± 38 at maximum metabolic activity after 11 hours, with elevated levels of Asp, Gly and Ala, and a reduction in Asn (Figure 4). In the oat-pea matrix, *Bacillus* did not significantly alter total free amino acid levels over time ($p = 1$, EMM).

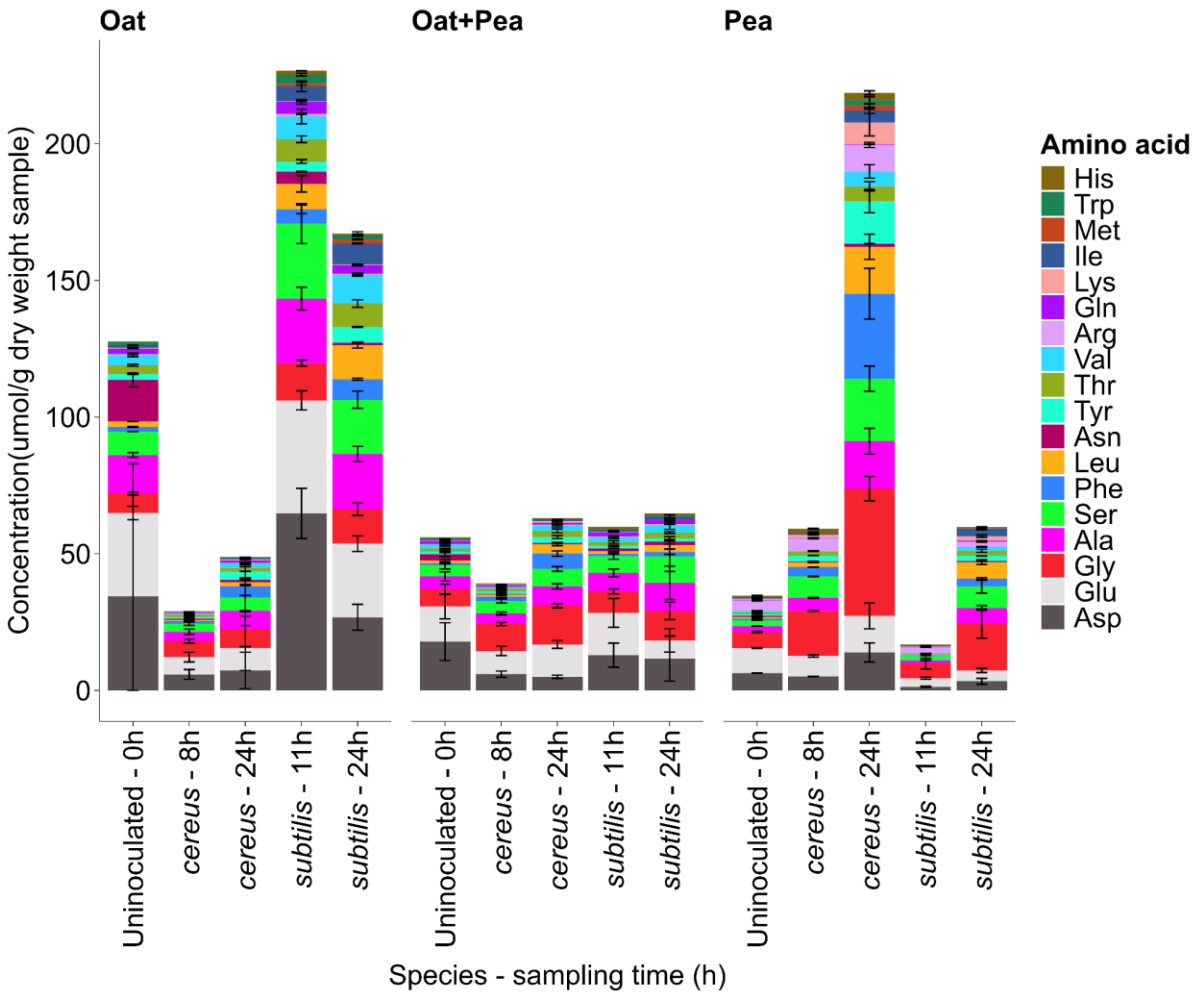

371 *Figure 6: Free amino acid profile of* Bacillus cereus *Y48H10 and* Bacillus subtilis *DSM21393*
372 *cultivated in oat, pea, and oat-pea matrices. Error bars are based on two biological replicates, each*
373 *consisting of four pooled technical replicates.*

374 Cereulide was exclusively quantified in the uninoculated matrices and in the *B. cereus* samples, since
375 it was assumed that *B. subtilis* is incapable of producing cereulide. Cereulide was below the detection
376 limit (0.1 ng/mL) in the pea matrix. In contrast, concentrations of 3.0 and 2.9 ng/mL were detected in
377 the oat-pea matrix, while the oat drink exhibited substantially higher concentrations of 46 and 48 ng/mL
378 in the two biological replicates.

379 **4. Discussion**

380 To examine the metabolic heat production of *B. cereus* and *B. subtilis*, a total of 24 *Bacillus* strains
381 were selected to represent diversity in origin, pathogenic potential, and genetic background. The
382 pathogenic potential - reflected in the ability to produce enterotoxins and/or emetic toxins (Table 1) -
383 was partially aligned with phylogenetic clustering, suggesting a link between genetic lineage and toxin
384 production capacity. All emetic strains showed the closest ANIm resemblance to *B. paranthracis*,
385 except for the emetic psychrotolerant strain, *B. mycoides* M67. Enterotoxin-producing strains were
386 identified in all three clades of the *B. cereus* group and could not be distinguished by phylogeny or
387 metabolic profiles. The classification of the strains within the *B. cereus* group (Table 1) reflects some
388 of the recent changes in the nomenclature of *Bacillus cereus* taxonomy. *B. wiedmannii* was proposed
389 as a new species in 2016 (Miller et al., 2016). *B. paranthracis, B. pacificus, and B. tropicus* were
390 proposed in 2017 (Liu et al., 2017), and *B. weihenstephanensis* merged with *B. mycoides* in 2018 (Liu
391 et al., 2018).

392 Clade-specific growth dynamics were observed in all Gompertz parameters during cultivation in BHI
393 at 30°C. *B. subtilis* exhibited a higher model-estimated total heat output (2745 mJ) than the observed
394 value (2473 mJ), indicating sustained metabolic activity beyond the 20-hour endpoint. In contrast, *B.*
395 *cereus* reached a metabolic plateau earlier, with modelled (1941 mJ) and measured (2000 mJ) values
396 closely aligned. Both species displayed a shoulder peak following the main heat flow peak (Figure 2B),
397 likely reflecting a shift in substrate utilization. Notably, *B. cereus* strains had a significantly shorter lag
398 phase (4.3 h ± 0.8) compared to *B. subtilis* (7.9 h ± 1.0), with no overlap observed between clades.

399 The observed differences in metabolic growth profiles may reflect the distinct ecological strategies of
400 each species in a highly nutrient-rich context, such as BHI medium. It is plausible that *B. subtilis*
401 exhibited more sustained metabolic activity and higher heat output in BHI due to a broader capacity for
402 peptide and carbohydrate catabolism, potentially supported by a diverse enzymatic repertoire. In
403 contrast, the rapid onset and early saturation of metabolic activity observed in *B. cereus* may reflect a
404 faster environmental adaptation coupled with a less energetically intensive growth strategy in nutrient-

405 rich conditions. Phylogenetic variation within each species further influenced metabolic heat production
406 in the BHI medium. *B. mycoides* (clade B) strains, for instance, released significantly less heat than
407 other *B. cereus* clades. This behaviour is consistent with the known psychrotolerant phenotype of one
408 of its members (MC67) and reduced growth at mesophilic temperatures (Guinebretière et al., 2008).

409 The influence of substrate composition on *Bacillus* growth dynamics became more apparent when
410 strains were cultivated in food matrices. To evaluate whether clade-specific metabolic traits persisted
411 across different food matrices, three strains of each of *Bacillus cereus* and *Bacillus subtilis* were
412 cultivated in milk, oat, pea, and a combined oat-pea matrix. As observed in BHI medium, *B. subtilis*
413 generally exhibited longer lag times than *B. cereus*, most notably in milk (12.4 hours vs. 7.4 hours).
414 However, species-level distinctions were less pronounced in the food matrices compared to BHI,
415 suggesting that substrate composition exerts a stronger influence on physiological responses than
416 phylogenetic background. The oat-pea matrix stood out as particularly supportive of *Bacillus* activity,
417 with the highest maximum calorimetric growth rate observed among all tested substrates. This suggests
418 that the combination of oat and pea provides a more favourable nutrient environment than either
419 substrate alone.

420 To elucidate the biochemical mechanisms underlying matrix-dependent growth dynamics, we analysed
421 sugar, organic acid, and free amino acid profiles during cultivation of one representative strain of each
422 *B. cereus* and *B. subtilis* in oat, pea, and oat-pea matrices. Despite the controlled experimental setup,
423 direct comparison of metabolic profiles across matrices was complicated by differences in thermal
424 treatment. The oat drink was not autoclaved, as preliminary experiments showed that heat treatment
425 inhibited *B. cereus* growth, likely due to degradation of heat-sensitive nutrients such as free amino
426 acids. In contrast, autoclaving was necessary to solubilize the pea hydrolysate in the pea and oat-pea
427 matrices. This discrepancy introduces a confounding variable, as thermal processing can trigger
428 Maillard reactions that reduce the availability of amino acids and simple sugars and alter the redox
429 balance (Lund & Ray, 2017). These effects may explain the elevated free amino acid levels observed
430 in the non-autoclaved oat matrix compared to the autoclaved pea-based matrices.

431 Despite these limitations, clear trends emerged in how matrix composition shaped metabolic activity.
432 The pea matrix, characterised by its low sugar content and the unique presence of citrate, showed clear
433 separation from oat and oat-pea in PCA. During cultivation on pea, both *B. cereus* and *B. subtilis*
434 produced and consumed organic acids, but their metabolic patterns diverged. *B. cereus* produced more
435 acetic acid than *B. subtilis* at the end of metabolism (24 hours). While citrate levels did not significantly
436 change during *B. cereus* metabolism in pea. *B. subtilis* reduced citrate levels, consistent with adaptive
437 citrate fermentation under nutrient stress or acidic conditions (Schilling et al., 2007). These species-
438 specific responses suggest that sugar limitation in pea may drive differential organic acid turnover. The
439 oat-pea matrix, which combines carbohydrate-rich and peptide-rich components, supported the most

440 pronounced accumulation of organic acids, including lactic acid and acetic acid, across both *Bacillus*
441 species. This suggests that the combined matrix could promote more efficient carbohydrate metabolism,
442 likely due to synergistic interactions between sugars and peptides, and may account for the higher
443 calorimetric growth observed in oat-pea.

444 Distinct species-specific strategies also emerged in the dynamics of free amino acids, revealing how *B.*
445 *cereus* and *B. subtilis* differentially interact with their nutrient environments. *B. subtilis* showed
446 transient free amino acid release in oat, consistent with its capacity to metabolize complex
447 carbohydrates and synthesize amino acids under nutrient-rich conditions. In contrast, *B. cereus*
448 accumulated free amino acids in the pea matrix, likely reflecting proteolytic activity and amino acid
449 catabolism under nutrient or oxygen stress. The limited changes of free amino acid levels in the oat-pea
450 matrix, despite high organic acid production, may indicate a metabolic shift away from amino acid
451 turnover toward carbohydrate fermentation. These observations align with previous findings that *B.*
452 *cereus* preferentially utilizes proteinaceous substrates under limited oxygen conditions (Chang et al.,
453 2021).

454 Cereulide, the heat- and acid-stable emetic toxin produced by *B. cereus*, was quantified across the food
455 matrices. The toxin was detected in both oat and oat-pea matrices, but not in pea, suggesting that matrix
456 composition influences toxin production—likely through differences in nutrient availability.
457 Interestingly, although *B. cereus* Y48H10 exhibited the highest heat production in the oat-pea matrix,
458 cereulide levels were lower than in oat alone. Ellouze et al. (2021), using *B. cereus* F4810/72, similarly
459 observed faster cereulide formation in a cereal-based matrix (rice) compared to a vegetable matrix
460 (vegetables purée) despite slower bacterial growth in the cereal-based matrix, supporting the notion that
461 cereulide production is matrix-dependent. However, in contrast to their findings on the vegetable
462 matrix, our study detected no quantifiable cereulide in pea at 30°C within 24 hours. High sugar and acid
463 levels in oats may enhance ATP availability, thereby favouring cereulide production (Marxen et al.,
464 2015). Previous studies have shown that cereulide expression is highly sensitive to environmental
465 factors, including pH, nutrient profile, and redox state (Dommel et al., 2010; Ehling-Schulz et al., 2015).
466 The absence of cereulide in pea and lower cereulide levels in oat-pea, despite microbial activity, may
467 reflect an indirect inhibitory effect of matrix composition on regulatory networks involved in cereulide
468 biosynthesis.

469 Whether components in pea actively suppress cereulide biosynthesis or limit precursor availability
470 remains unresolved and warrants further investigation. While cereulide is typically associated with
471 starchy foods (Messelhäusser et al., 2014), outbreaks have been reported in legume-based products such
472 as fermented soybeans (Inatsu et al., 2020) and soaked navy beans (Nicholls et al., 2016), indicating
473 that low-carbohydrate environments can support toxin synthesis under permissive conditions. Thorsen
474 et al. (2011) found no emetic strains in a survey of African bread snacks made from legumes, whereas

Kyrylenko et al. (2023) reported that 9% of *B. cereus* isolates from plant-based dairy alternative ingredients carried cereulide-producing genes. These findings highlight the variability in risk across substrates and reinforce the importance of matrix-specific evaluations when assessing cereulide-associated hazards.

Metabolic heat profiling provided complementary insights into *Bacillus* physiology, distinguishing species- and clade-level behaviour under controlled conditions. Our findings reveal that *B. subtilis* consistently produces more metabolic heat than *B. cereus*. Differences in lag time and growth rate were matrix-dependent, highlighting the limitations of extrapolating from defined media, such as BHI. Although calorimetry alone cannot resolve underlying metabolic pathways, its integration with metabolomic profiling offers a robust framework for assessing microbial activity, adaptation, and potential safety risks in complex food systems. While the metabolic capacities of *B. subtilis* and *B. cereus* are well-characterized in defined media, their proteomic responses in food matrices remain underexplored (Wicke et al., 2023). Future studies integrating calorimetry, metabolomics, and proteomics could help uncover matrix-specific regulatory mechanisms that govern spoilage activity and beneficial fermentation traits in *B. subtilis*, as well as toxin production and contamination risks associated with *B. cereus*. Such approaches are essential for understanding *Bacillus* behaviour in diverse food environments.

5. Conclusion

This study demonstrates that *Bacillus cereus* and *Bacillus subtilis* exhibit distinct metabolic behaviour across food-relevant matrices. In BHI at 30°C, *B. subtilis* showed longer lag times and higher total heat production than *B. cereus*. However, in food matrices, substrate composition had a more pronounced effect on metabolic activity than species identity, although *B. subtilis* consistently generated more heat overall.

The combined oat-pea matrix supported the highest calorimetric growth rates, likely driven by enhanced carbohydrate metabolism, as evidenced by reduced sugar levels and increased organic acids. In contrast, the pea matrix- characterised by low sugar and the unique presence of citrate, triggered post-metabolic consumption of citrate by *B. subtilis*. Free amino acid profiles reflected matrix-specific strategies, *B. subtilis* released free amino acids in oat, while *B. cereus* predominantly did so in pea. Interestingly, despite high calorimetric activity, the oat-pea matrix showed limited change in free amino acid levels, suggesting a shift toward carbohydrate-driven metabolism.

Cereulide production by *B. cereus* was strongly matrix-dependent, with high levels detected in oat, moderate levels in oat-pea, and none in pea, highlighting the role of substrate composition in toxin synthesis. Together, these findings underscore the need for matrix-specific microbial risk assessment

tools. They also demonstrate that integration of isothermal microcalorimetry with metabolomics provides a more nuanced understanding of microbial behaviour in complex food environments. Similar heat profiles can mask divergent metabolic strategies; thus, this combined approach offers a valuable tool for evaluating spoilage and contamination risks, particularly in the development of safer plant-based food products.

Acknowledgment

The authors wish to acknowledge the Villum Foundation (HLR:34434) and the joint alliance grant between the Danish Dairy Research Foundation, Arla Foods amba, Novonesis, and the University of Copenhagen (SK: SaFeMix) for financial support.

Conflict of interest

The authors declare that they have no known competing financial interests or other conflicts of interest.

Author contribution

Emilie V. Skriver: Conceptualization, Methodology, Formal analysis, Investigation, Visualization, Writing – original draft, Writing – review and editing; Tessa S. Canoy: Conceptualization, Methodology, Formal analysis, Investigation, Visualization, Writing – original draft, Writing – review and editing; Yuandong Sha: Formal analysis, Investigation, Visualization; Morten A. Rasmussen: Software, Formal analysis; Bekzod Khakimov: Methodology, Formal analysis, Supervision; Susanne Knøchel: Writing – review and editing, Resources, Supervision, Project administration, Funding acquisition; Henriette L. Røder; Conceptualization, Methodology, Resources, Writing – review and editing, Supervision, Project administration, Funding acquisition.

References

Anonymous. (2017). ISO18465: *Microbiology of the food chain-Quantitative determination of emetic toxin (cereulide) using LC-MS/MS COPYRIGHT PROTECTED DOCUMENT*. www.iso.org

Beilharz, K., Kragh, K. N., Fritz, B., Kirkegaard, J. B., Tolker-Nielsen, T., Bjarnsholt, T., & Lichtenberg, M. (2023). Protocol to assess metabolic activity of Pseudomonas aeruginosa by measuring heat flow using isothermal calorimetry. *STAR Protocols*, *4*(2). https://doi.org/10.1016/j.xpro.2023.102269

Braissant, O., Wirz, D., Göpfert, B., & Daniels, A. U. (2010). Use of isothermal microcalorimetry to monitor microbial activities [Article]. *FEMS Microbiology Letters*, *303*(1), 1–8. https://doi.org/10.1111/j.1574-6968.2009.01819.x

Carroll, L. M., Cheng, R. A., Wiedmann, M., & Kovac, J. (2022). Keeping up with the Bacillus cereus group: taxonomy through the genomics era and beyond. In *Critical Reviews in Food Science and*

Nutrition (Vol. 62, Issue 28, pp. 7677–7702). Taylor and Francis Ltd. https://doi.org/10.1080/10408398.2021.1916735

Chang, J. D., Vaughan, E. E., Liu, C. G., Jelinski, J. W., Terwilliger, A. L., & Maresso, A. W. (2021). Metabolic profiling reveals nutrient preferences during carbon utilization in Bacillus species [Article]. *Scientific Reports*, *11*(1), 23917–23917. https://doi.org/10.1038/s41598-021-03420-7

Cichos, K. H., Ruark, R. J., & Ghanem, E. S. (2023). Isothermal microcalorimetry improves accuracy and time to bacterial detection of periprosthetic joint infection after total joint arthroplasty [Article]. *Journal of Clinical Microbiology*, *61*(12), e0089323–e0089323. https://doi.org/10.1128/jcm.00893-23

Dommel, M. K., Frenzel, E., Strasser, B., Bloechinger, C., Scherer, S., & Ehling-Schulz, M. (2010). Identification of the Main Promoter Directing Cereulide Biosynthesis in Emetic Bacillus cereus and Its Application for Real-Time Monitoring of ces Gene Expression in Foods [Article]. *Applied and Environmental Microbiology*, *76*(4), 1232–1240. https://doi.org/10.1128/AEM.02317-09

Dong, H., Zhu, H., He, H., & Yi, C. (2023). Identification and evaluation of spoilage potential of four Bacillus strains isolated from slimy rice noodles [Article]. *Food Microbiology*, *110*, 104160. https://doi.org/10.1016/j.fm.2022.104160

Earl, A. M., Losick, R., & Kolter, R. (2008). Ecology and genomics of Bacillus subtilis [Article]. *Trends in Microbiology (Regular Ed.)*, *16*(6), 269–275. https://doi.org/10.1016/j.tim.2008.03.004

EFSA. (2022). The European Union One Health 2021 Zoonoses Report. *EFSA Journal*, *20*(12). https://doi.org/10.2903/j.efsa.2022.7666

Ehling-Schulz, M., Frenzel, E., & Gohar, M. (2015). Food-bacteria interplay: Pathometabolism of emetic Bacillus cereus. *Frontiers in Microbiology*, *6*(JUN). https://doi.org/10.3389/fmicb.2015.00704

Ehling-Schulz, M., Fricker, M., & Scherer, S. (2004). Bacillus cereus, the causative agent of an emetic type of food-borne illness [Article]. *Molecular Nutrition & Food Research*, *48*(7), 479–487. https://doi.org/10.1002/mnfr.200400055

Ellouze, M., Buss Da Silva, N., Rouzeau-Szynalski, K., Coisne, L., Cantergiani, F., & Baranyi, J. (2021). Modeling Bacillus cereus Growth and Cereulide Formation in Cereal-, Dairy-, Meat-, Vegetable-Based Food and Culture Medium. *Frontiers in Microbiology*, *12*. https://doi.org/10.3389/fmicb.2021.639546

Guinebretière, M. H., Thompson, F. L., Sorokin, A., Normand, P., Dawyndt, P., Ehling-Schulz, M., Svensson, B., Sanchis, V., Nguyen-The, C., Heyndrickx, M., & De Vos, P. (2008). Ecological diversification in the Bacillus cereus Group. *Environmental Microbiology*, *10*(4), 851–865. https://doi.org/10.1111/j.1462-2920.2007.01495.x

Inatsu, Y., Chotiko, A., & Nanchaipattana, C. (2020). Contaminated Bacillus cereus in Lao and Thai fermented soybean "Tua Nao." *Japan Agricultural Research Quarterly*, *54*(1), 47–51. https://doi.org/10.6090/jarq.54.47

Kahm, M., Hasenbrink, G., Lichtenberg-Frate, H., Ludwig, J., & Kschischo, M. (2010). grofit: Fitting Biological Growth Curves with R [Article]. *Journal of Statistical Software*, *33*(7), 1–21. https://doi.org/10.18637/jss.v033.i07

Kpikpi, E. N., Thorsen, L., Glover, R., Dzogbefia, V. P., & Jespersen, L. (2014). Identification of Bacillus species occurring in Kantong, an acid fermented seed condiment produced in Ghana [Article]. *International Journal of Food Microbiology*, *180*, 1–6. https://doi.org/10.1016/j.ijfoodmicro.2014.03.028

Kyrylenko, A., Eijlander, R. T., Alliney, G., de Bos, E. L. van, & Wells-Bennik, M. H. J. (2023). Levels and types of microbial contaminants in different plant-based ingredients used in dairy

alternatives. *International Journal of Food Microbiology*, *407*. https://doi.org/10.1016/j.ijfoodmicro.2023.110392

Li, Z., Zheng, M., Zheng, J., & Gänzle, M. G. (2023). Bacillus species in food fermentations: an underappreciated group of organisms for safe use in food fermentations [Article]. *Current Opinion in Food Science*, *50*, 101007. https://doi.org/10.1016/j.cofs.2023.101007

Lichtenberg, M., Kvich, L., Larsen, S. L. B., Jakobsen, T. H., & Bjarnsholt, T. (2022). Inoculum Concentration Influences Pseudomonas aeruginosa Phenotype and Biofilm Architecture [Article]. *Microbiology Spectrum*, *10*(6). https://doi.org/10.1128/spectrum.03131-22

Liu, Y., Du, J., Lai, Q., Zeng, R., Ye, D., Xu, J., & Shao, Z. (2017). Proposal of nine novel species of the Bacillus cereus group [Article]. *International Journal of Systematic and Evolutionary Microbiology*, *67*(8), 2499–2508. https://doi.org/10.1099/ijsem.0.001821

Liu, Y., Lai, Q., & Shao, Z. (2018). Genome analysis-based reclassification of Bacillus weihenstephanensis as a later heterotypic synonym of Bacillus mycoides [Article]. *International Journal of Systematic and Evolutionary Microbiology*, *68*(1), 106–112. https://doi.org/10.1099/ijsem.0.002466

Lund, M. N., & Ray, C. A. (2017). Control of Maillard Reactions in Foods: Strategies and Chemical Mechanisms [Article]. *Journal of Agricultural and Food Chemistry*, *65*(23), 4537–4552. https://doi.org/10.1021/acs.jafc.7b00882

Marxen, S., Stark, T. D., Frenzel, E., Rütschle, A., Lücking, G., Pürstinger, G., Pohl, E. E., Scherer, S., Ehling-Schulz, M., & Hofmann, T. (2015). Chemodiversity of cereulide, the emetic toxin of Bacillus cereus. *Analytical and Bioanalytical Chemistry*, *407*(9), 2439–2453. https://doi.org/10.1007/s00216-015-8511-y

Messelhäusser, U., Frenzel, E., Blöchinger, C., Zucker, R., Kämpf, P., & Ehling-Schulz, M. (2014). Emetic Bacillus cereus are more volatile than thought: Recent foodborne outbreaks and prevalence studies in bavaria (2007-2013). *BioMed Research International*, *2014*. https://doi.org/10.1155/2014/465603

Miller, R. A., Beno, S. M., Kent, D. J., Carroll, L. M., Martin, N. H., Boor, K. J., & Kovac, J. (2016). Bacillus wiedmannii sp nov., a psychrotolerant and cytotoxic Bacillus cereus group species isolated from dairy foods and dairy environments [Article]. *International Journal of Systematic and Evolutionary Microbiology*, *66*(11), 4744–4753. https://doi.org/10.1099/ijsem.0.001421

Mozhaitseva, K., Pairaud, S., Firmesse, O., & Bonis, M. (2025). Population structure of Bacillus cereus sensu lato associated with foodborne outbreaks in France between 2004 and 2023 [Document]. *BioRxiv*. https://doi.org/10.1101/2025.03.24.644875

Na, S.-I., Kim, Y. O., Yoon, S.-H., Ha, S., Baek, I., & Chun, J. (2018). UBCG: Up-to-date bacterial core gene set and pipeline for phylogenomic tree reconstruction [Article]. *The Journal of Microbiology*, *56*(4), 280–285. https://doi.org/10.1007/s12275-018-8014-6

Nicholls, M., Purcell, B., Willis, C., Amar, C. F. L., Kanagarajah, S., Chamberlain, D., Woolridge, D., Morgan, J., McLauchlin, J., Grant, K. A., Harvey-Vince, L., Padfield, M., Mearkle, R., & Chow, J. Y. (2016). Investigation of an outbreak of vomiting in nurseries in South East England, May 2012 [Article]. *Epidemiology and Infection*, *144*(3), 582–590. https://doi.org/10.1017/S0950268815001491

Oren, A., Arahal, D. R., Göker, M., Moore, E. R. B., Rossello-Mora, R., & Sutcliffe, I. C. (2023). International Code of Nomenclature of Prokaryotes. Prokaryotic Code (2022 Revision) [Article]. *International Journal of Systematic and Evolutionary Microbiology*, *73*(5a). https://doi.org/10.1099/ijsem.0.005585

Owusu-Kwarteng, J., Parkouda, C., Adewumi, G. A., Ouoba, L. I. I., & Jespersen, L. (2022). Technologically relevant Bacillus species and microbial safety of West African traditional

alkaline fermented seed condiments [Article]. *Critical Reviews in Food Science and Nutrition*, *62*(4), 871–888. https://doi.org/10.1080/10408398.2020.1830026

Parkouda, C., Thorsen, L., Compaoré, C. S., Nielsen, D. S., Tano-Debrah, K., Jensen, J. S., Diawara, B., & Jakobsen, M. (2010). Microorganisms associated with Maari, a Baobab seed fermented product [Article]. *International Journal of Food Microbiology*, *142*(3), 292–301. https://doi.org/10.1016/j.ijfoodmicro.2010.07.004

Price, M. N., Dehal, P. S., & Arkin, A. P. (2010). FastTree 2-Approximately Maximum-Likelihood Trees for Large Alignments [Article]. *PloS One*, *5*(3), e9490–e9490. https://doi.org/10.1371/journal.pone.0009490

Rahnama, H., Azari, R., Yousefi, M. H., Berizi, E., Mazloomi, S. M., Hosseinzadeh, S., Derakhshan, Z., Ferrante, M., & Conti, G. O. (2023). A systematic review and meta-analysis of the prevalence of Bacillus cereus in foods [Article]. *Food Control*, *143*, 109250. https://doi.org/10.1016/j.foodcont.2022.109250

Rehlund, A. S. G., Canoy, T. S., Nielsen, D. S., Lund, M. N., & Poojary, M. M. (2025). Protein hydrolysis for amino acid analysis revisited. *Food Chemistry*, 146224.

Robas Mora, M., Fernández Pastrana, V. M., Oliva, L. L. G., Lobo, A. P., & Jiménez Gómez, P. A. (2023). Plant growth promotion of the forage plant Lupinus albus Var. Orden Dorado using Pseudomonas agronomica sp. nov. and Bacillus pretiosus sp. nov. added over a valorized agricultural biowaste [Article]. *Frontiers in Microbiology*, *13*, 1046201. https://doi.org/10.3389/fmicb.2022.1046201

Schilling, O., Frick, O., Herzberg, C., Ehrenreich, A., Heinzle, E., Wittmann, C., & Stülke, J. (2007). Transcriptional and Metabolic Responses of Bacillus subtilis to the Availability of Organic Acids: Transcription Regulation Is Important but Not Sufficient To Account for Metabolic Adaptation [Article]. *Applied and Environmental Microbiology*, *73*(2), 499–507. https://doi.org/10.1128/AEM.02084-06

Skriver, E. V., Canoy, T. S., Reilly, E. T., Gkogka, E., Lucena, D., Knøchel, S., & Lyng Røder, H. (2025). Whole genome sequences of 20 Bacillus cereus strains isolated from various environments. *Submitted to Publication*.

Snyder, A. B., Martin, N., & Wiedmann, M. (2024). Microbial food spoilage: impact, causative agents and control strategies [Article]. *Nature Reviews. Microbiology*, *22*(9), 528–542. https://doi.org/10.1038/s41579-024-01037-x

Sonenshein, A. L. (2007). Control of key metabolic intersections in Bacillus subtilis [Article]. *Nature Reviews. Microbiology*, *5*(12), 917–927. https://doi.org/10.1038/nrmicro1772

Tamura, K., Stecher, G., & Kumar, S. (2021). MEGA11: Molecular Evolutionary Genetics Analysis Version 11 [Article]. *Molecular Biology and Evolution*, *38*(7), 3022–3027. https://doi.org/10.1093/molbev/msab120

Thorsen, L., Abdelgadir, W. S., Rønsbo, M. H., Abban, S., Hamad, S. H., Nielsen, D. S., & Jakobsen, M. (2011). Identification and safety evaluation of Bacillus species occurring in high numbers during spontaneous fermentations to produce Gergoush, a traditional Sudanese bread snack [Article]. *International Journal of Food Microbiology*, *146*(3), 244–252. https://doi.org/10.1016/j.ijfoodmicro.2011.02.028

Thorsen, L., Azokpota, P., Hansen, B. M., Hounhouigan, D. J., & Jakobsen, M. (2010). Identification, genetic diversity and cereulide producing ability of Bacillus cereus group strains isolated from Beninese traditional fermented food condiments [Article]. *International Journal of Food Microbiology*, *142*(1), 247–250. https://doi.org/10.1016/j.ijfoodmicro.2010.06.004

UNEP. (2024). *Food Waste Index Report 2024. Think Eat Save: Tracking Progress to Halve Global Food Waste.* https://wedocs.unep.org/20.500.11822/45230.

Valerio, F., De Bellis, P., Lonigro, S. L., Visconti, A., & Lavermicocca, P. (2008). Use of Lactobacillus plantarum fermentation products in bread-making to prevent Bacillus subtilis ropy spoilage [Article]. *International Journal of Food Microbiology*, *122*(3), 328–332. https://doi.org/10.1016/j.ijfoodmicro.2008.01.005

Wicke, D., Meißner, J., Warneke, R., Elfmann, C., & Stülke, J. (2023). Understudied proteins and understudied functions in the model bacterium Bacillus subtilis—A major challenge in current research [Article]. *Molecular Microbiology*, *120*(1), 8–19. https://doi.org/10.1111/mmi.15053

Wiedenbein, E. S., Canoy, T. S., Hui, Y., Parkouda, C., Compaoré, C. S., Ametefe, E., Jakobsen, M., Jespersen, L., & Nielsen, D. S. (2023). Complete and Draft Genome Sequences of 52 Bacillus and Priestia Strains Isolated from West African Fermentations and 26 Reference Strains from a Public Culture Collection . *Microbiology Resource Announcements*, *12*(7). https://doi.org/10.1128/mra.00394-23

Zwietering, M. H., Jongenburger, I., Rombouts, F. M., & Vantriet, K. (1990). Modeling of the Bacterial Growth Curve [Article]. *Applied and Environmental Microbiology*, *56*(6), 1875–1881. https://doi.org/10.1128/aem.56.6.1875-1881.1990

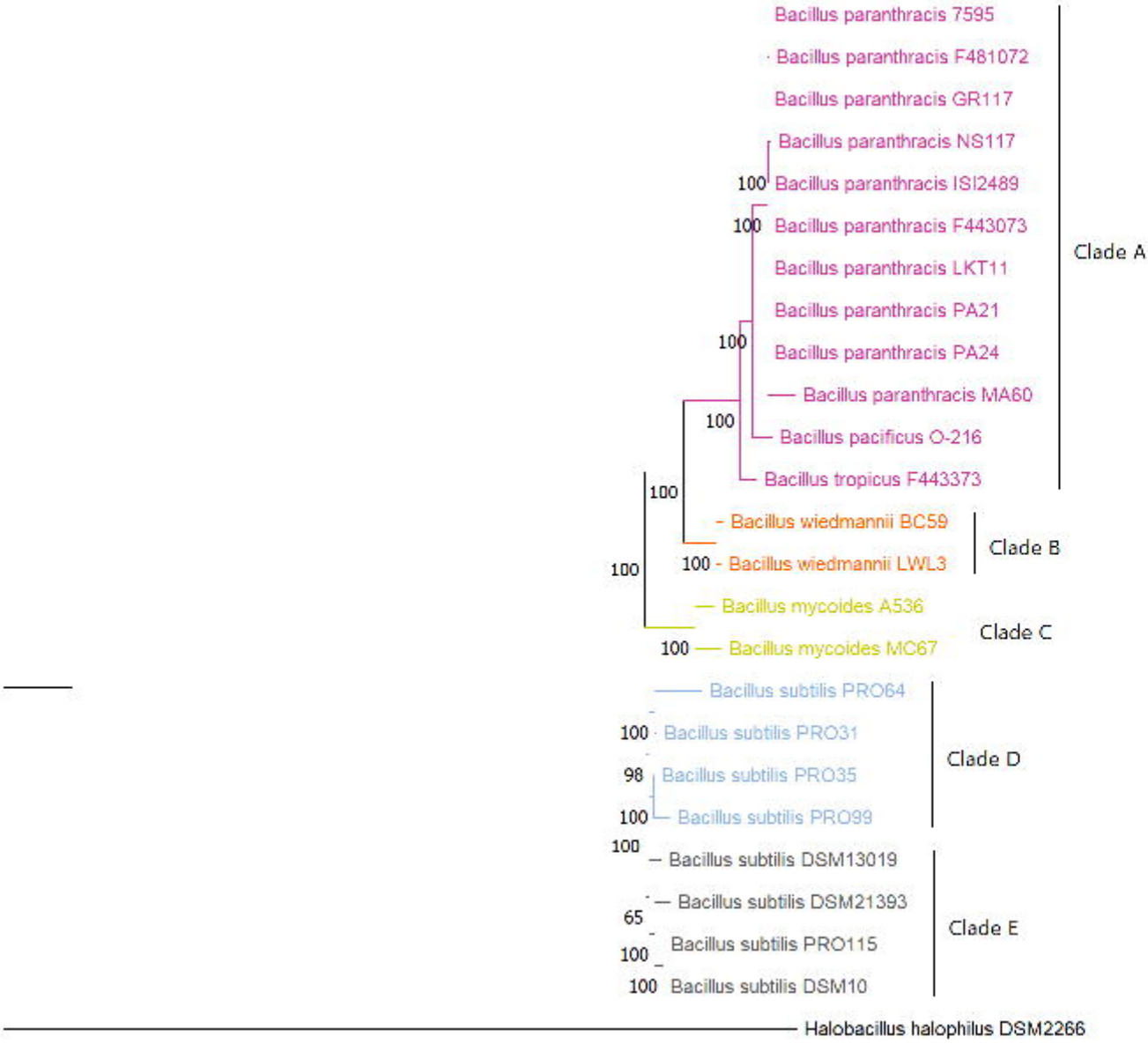
Bacillus paranthracis 7595
Bacillus paranthracis F481072
Bacillus paranthracis GR117
Bacillus paranthracis NS117
100
Bacillus paranthracis ISI2489
100
Bacillus paranthracis F443073
Bacillus paranthracis LKT11
Bacillus paranthracis PA21
100
Bacillus paranthracis PA24
Bacillus paranthracis MA60
100
Bacillus pacificus O-216
Bacillus tropicus F443373
Clade A
100
Bacillus wiedmannii BC59
100
Bacillus wiedmannii LWL3
Clade B
100
Bacillus mycoides A536
100
Bacillus mycoides MC67
Clade C
Bacillus subtilis PRO64
100
Bacillus subtilis PRO31
98
Bacillus subtilis PRO35
100
Bacillus subtilis PRO99
Clade D
100
Bacillus subtilis DSM13019
Bacillus subtilis DSM21393
65
Bacillus subtilis PRO115
100
100
Bacillus subtilis DSM10
Clade E
Halobacillus halophilus DSM2266

(A) Sugars

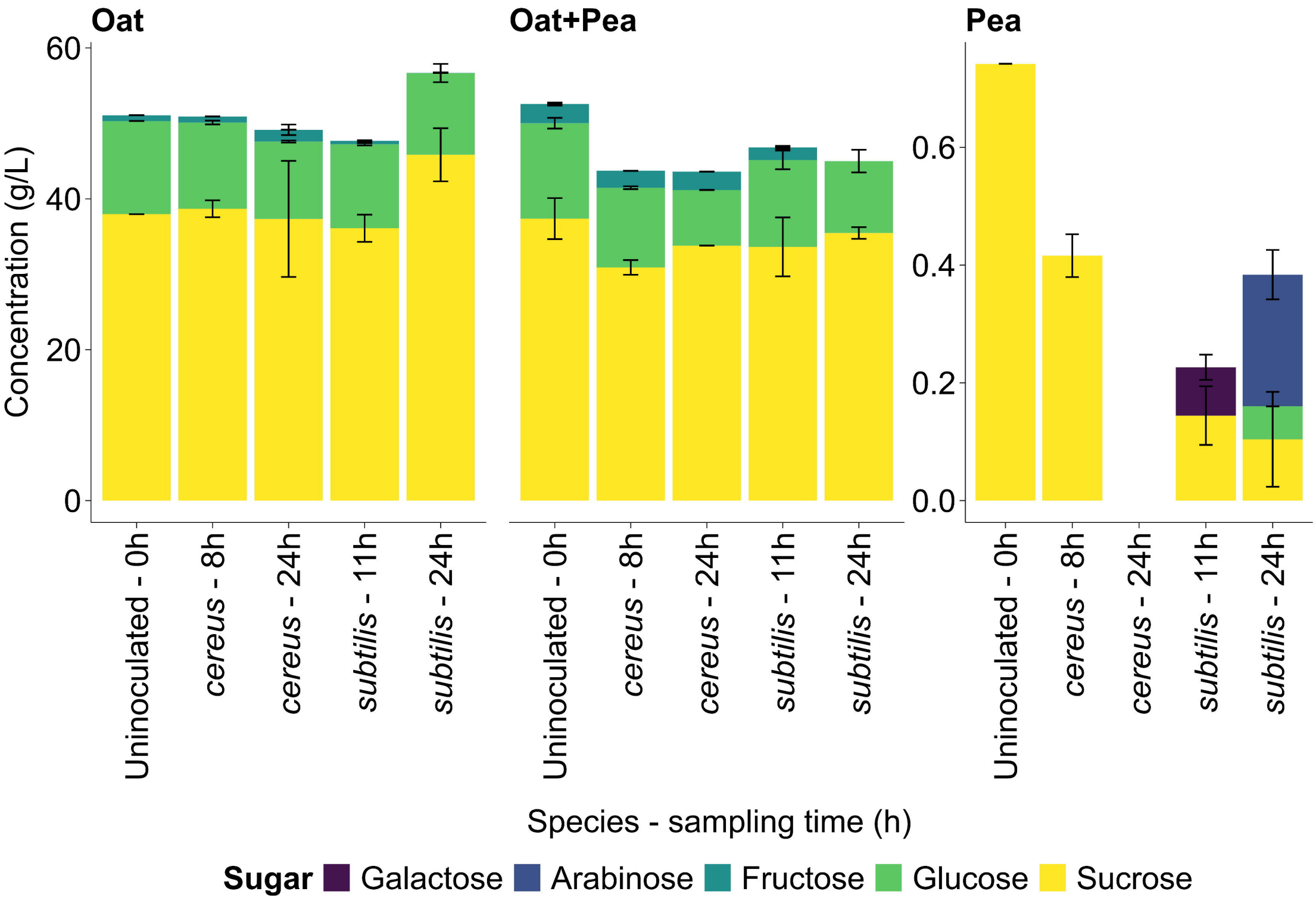

(B) Organic acids

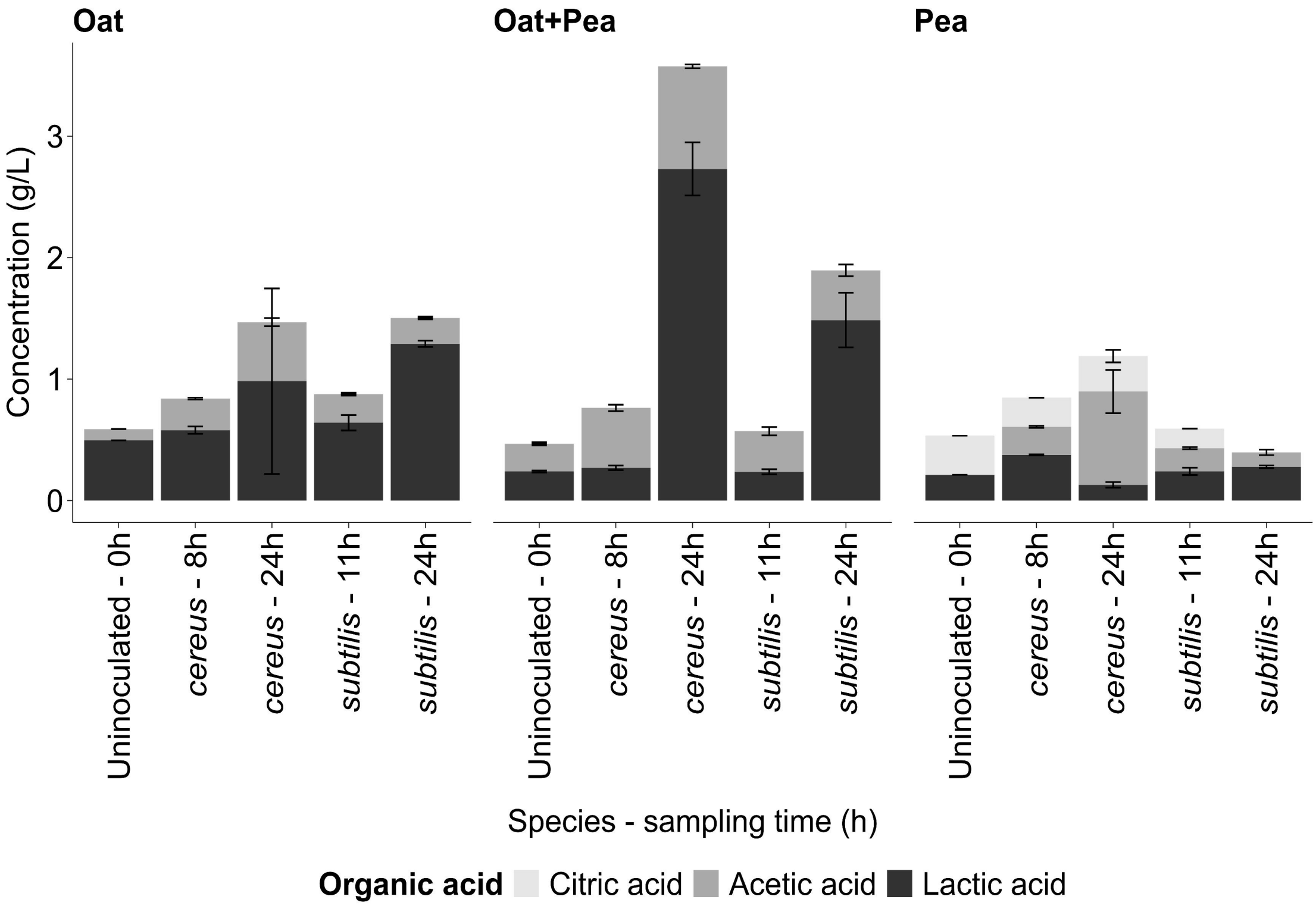

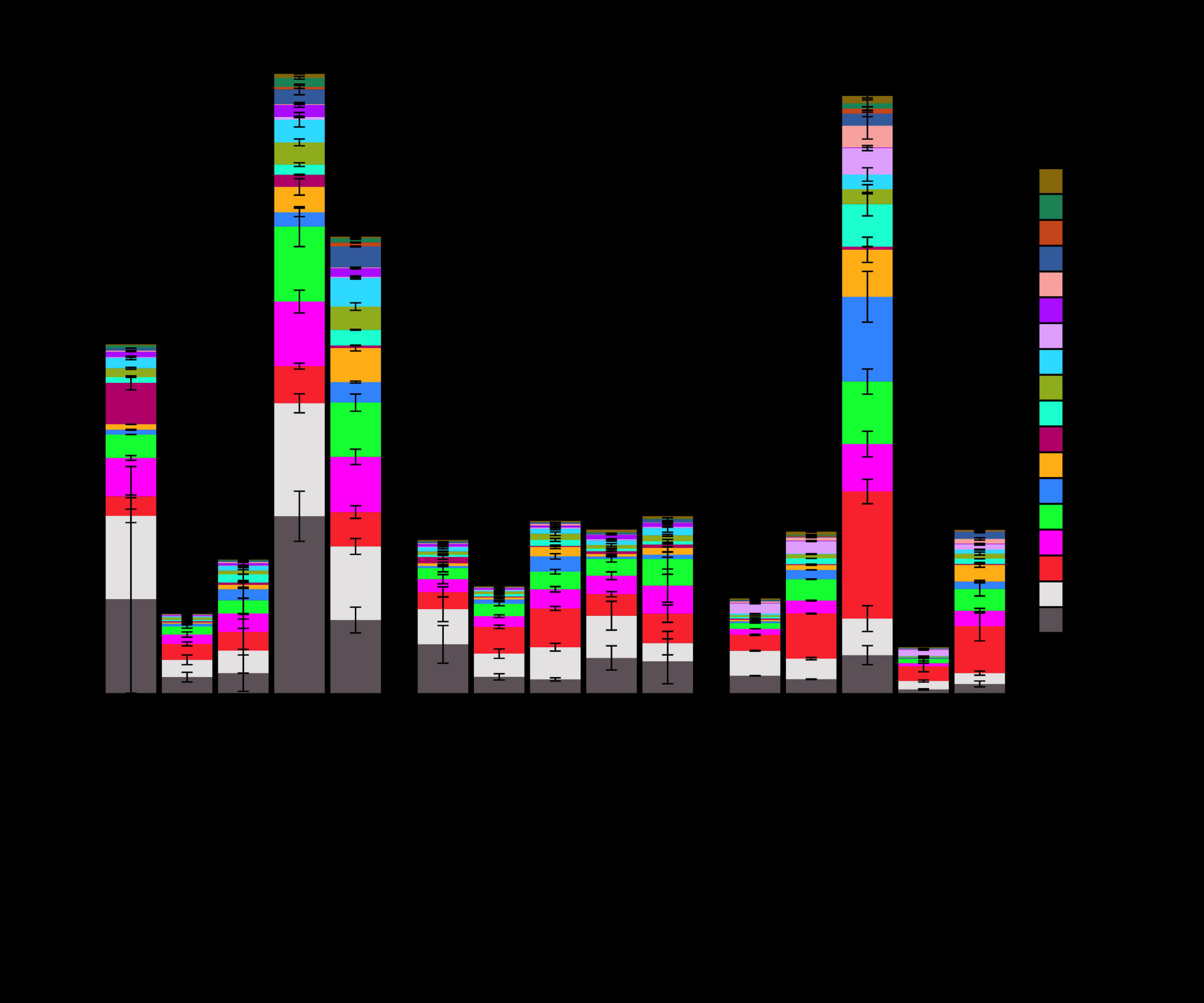

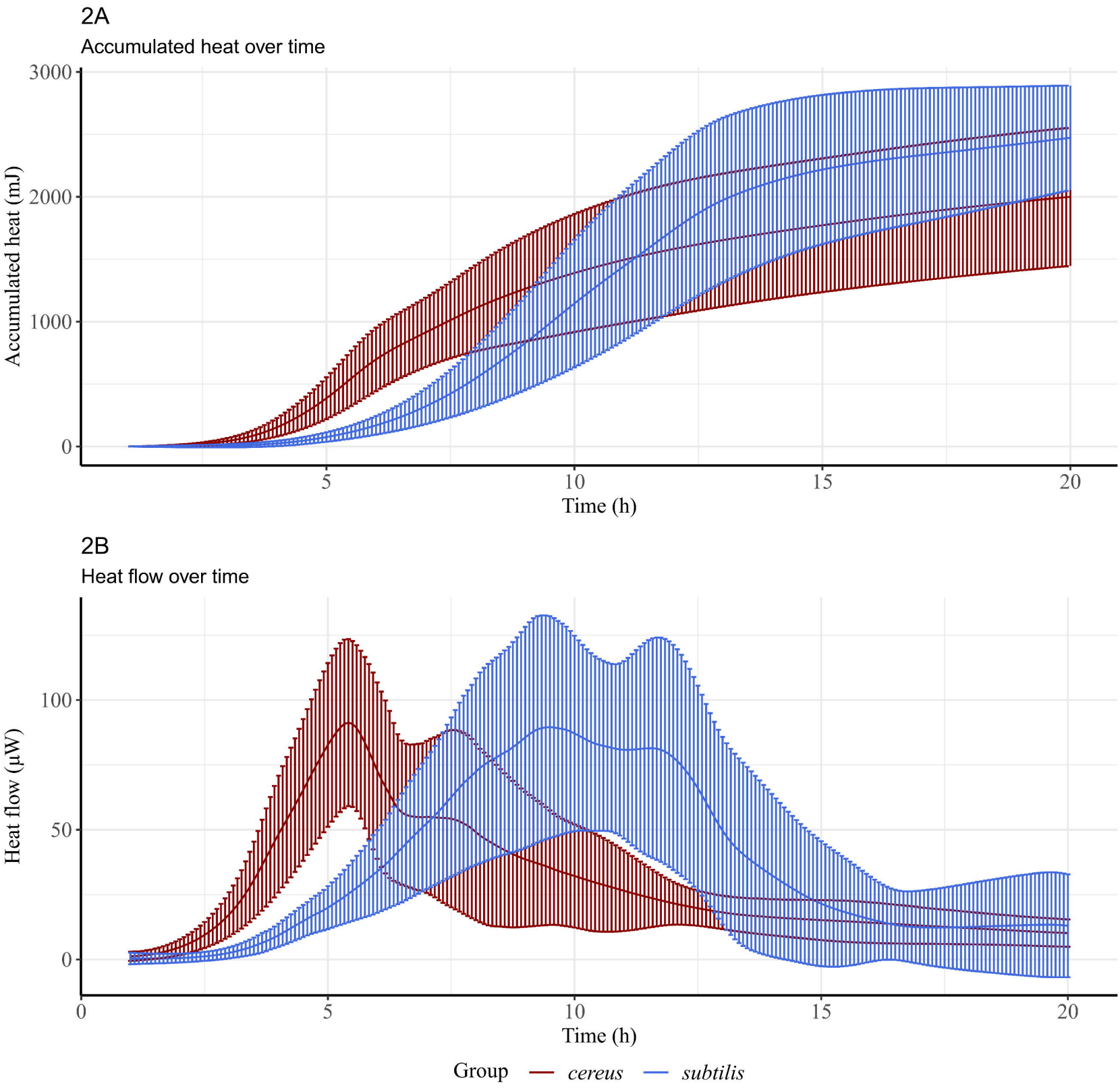
2A
Accumulated heat over time
Accumulated heat (mJ)
3000
2000
1000
0
5
10
15
20
Time (h)
2B
Heat flow over time
Heat flow (μW)
100
50
0
0
5
10
15
20
Time (h)
Group
cereus
subtilis

A

Comparison of Gompertz heat parameters between *Bacillus cereus* and *Bacillus subtilis*

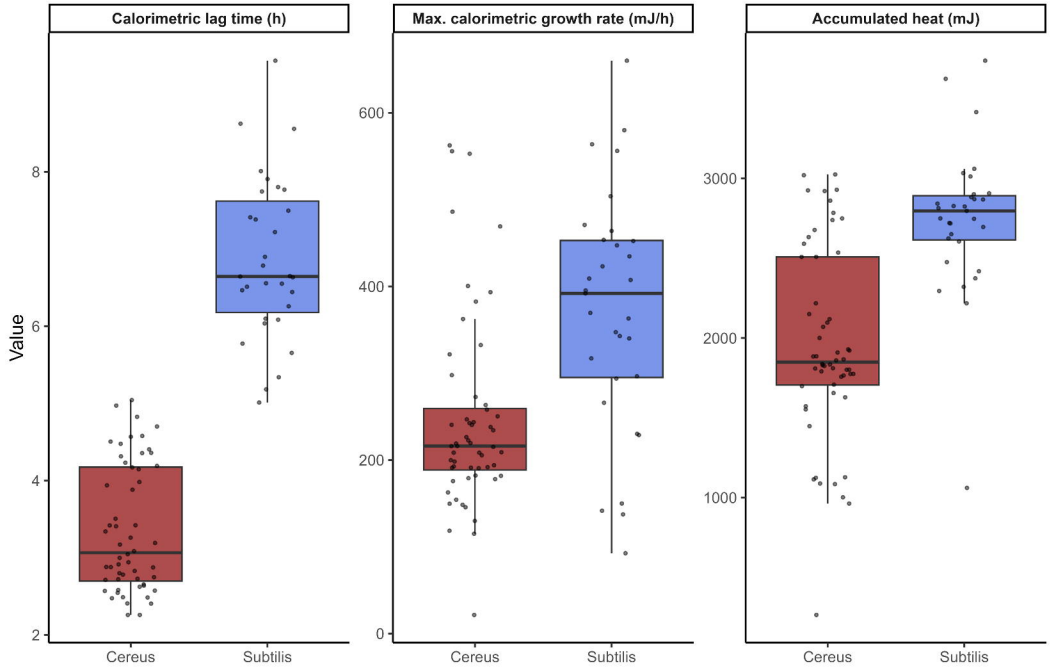

B

Comparison of Gompertz heat parameters within *Bacillus cereus* and within *Bacillus subtilis* clades

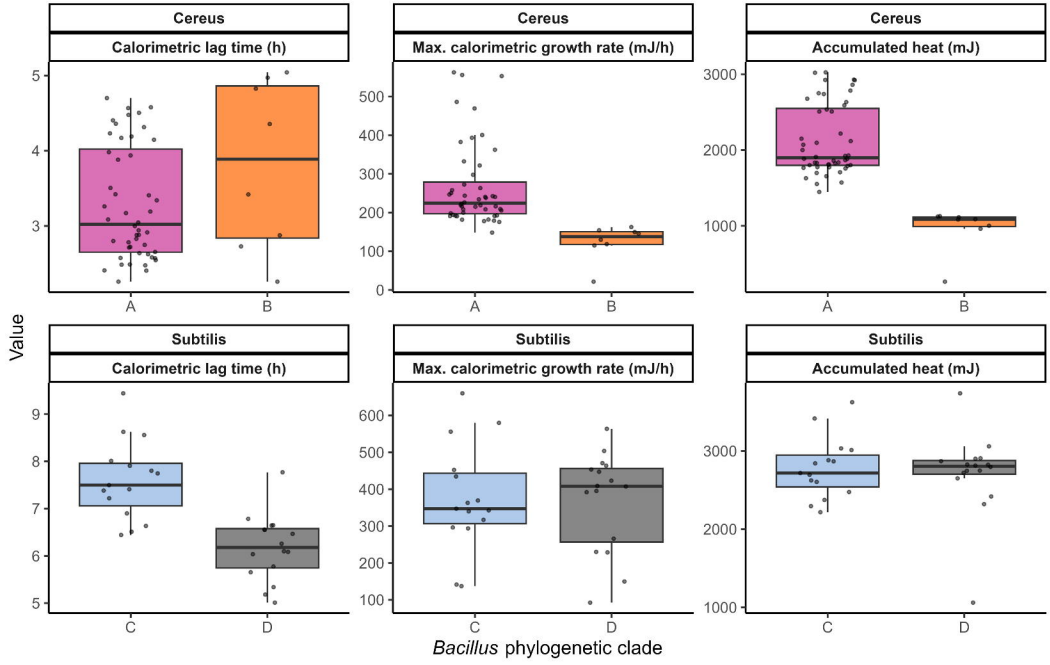
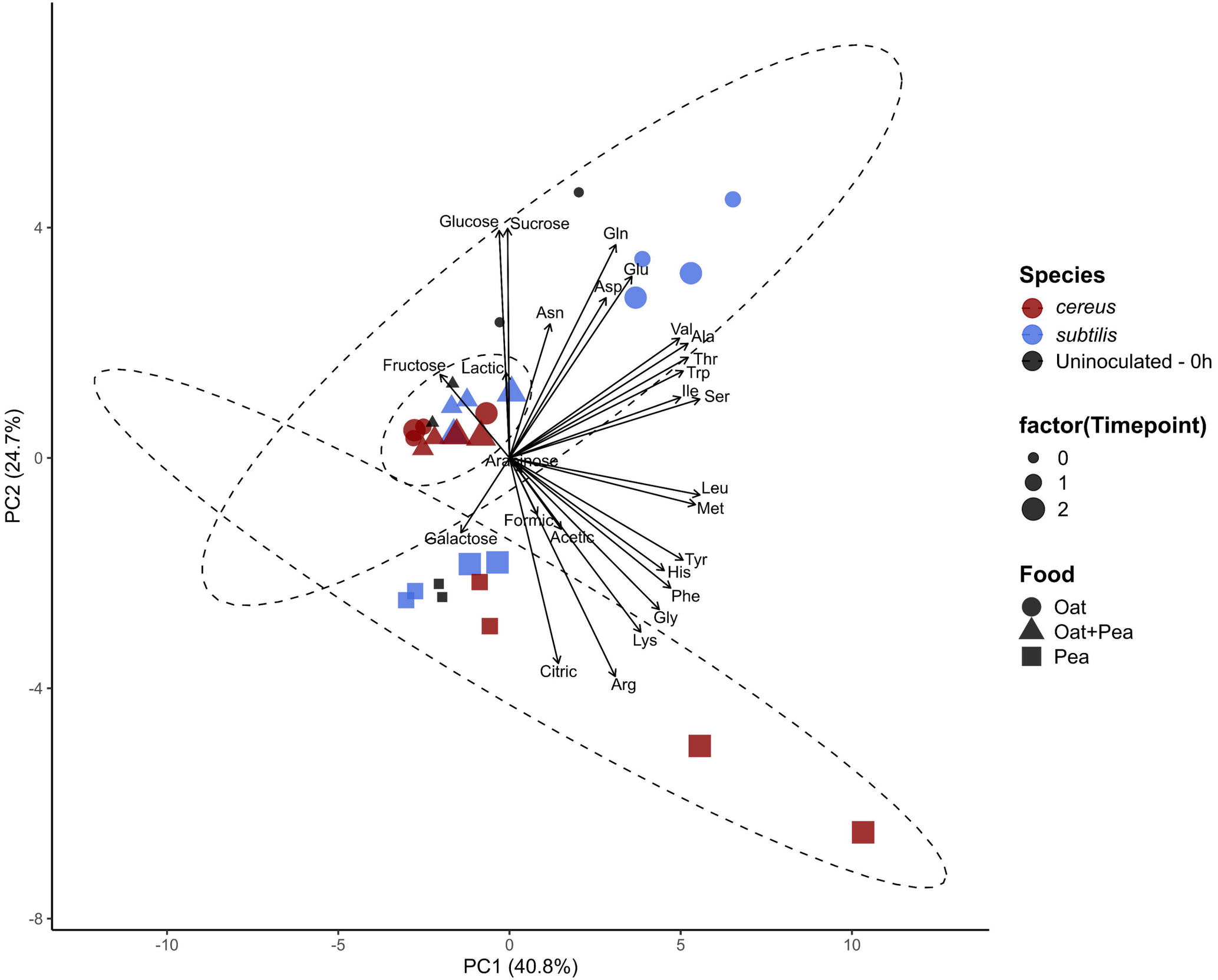
Combined Metabolite Analysis